XIII International Conference on New Frontiers in Physics
26 Aug - 4 Sep 2024, OAC, Kolymbari, Crete, Greece

STAR (non-spin) Highlights

Barbara Trzeciak, for the STAR Collaboration
Czech Technical University in Prague

Supported in part by
U.S. DEPARTMENT OF ENERGY | Office of Science

CTU CZECH TECHNICAL UNIVERSITY IN PRAGUE

Outline

1 STAR detector and physics program

2 QCD phase diagram and QGP properties

- Critical point, Collectivity, Vorticity, Strangeness, Dielectrons, Quarkonia

3 Particle production

- Light (hyper-)nuclei production, Baryon number carrier

4 Detector upgrades and future

STAR talks at the ICNFP Conference:

STAR Correlations, Fluctuations
Yu Hu

STAR Flow, Chirality, Vorticity
Yicheng Feng

STAR CME in Isobars
Jagbir Singh

STAR Jet Highlights
Tanmay Pani

STAR Spin Highlights
Ting Lin

STAR Forward Spin Physics
Xilin Liang

STAR detector at RHIC

- Wide range of collision beam energies
- Different collision species at the top RHIC energy
- Increase in statistics over the years

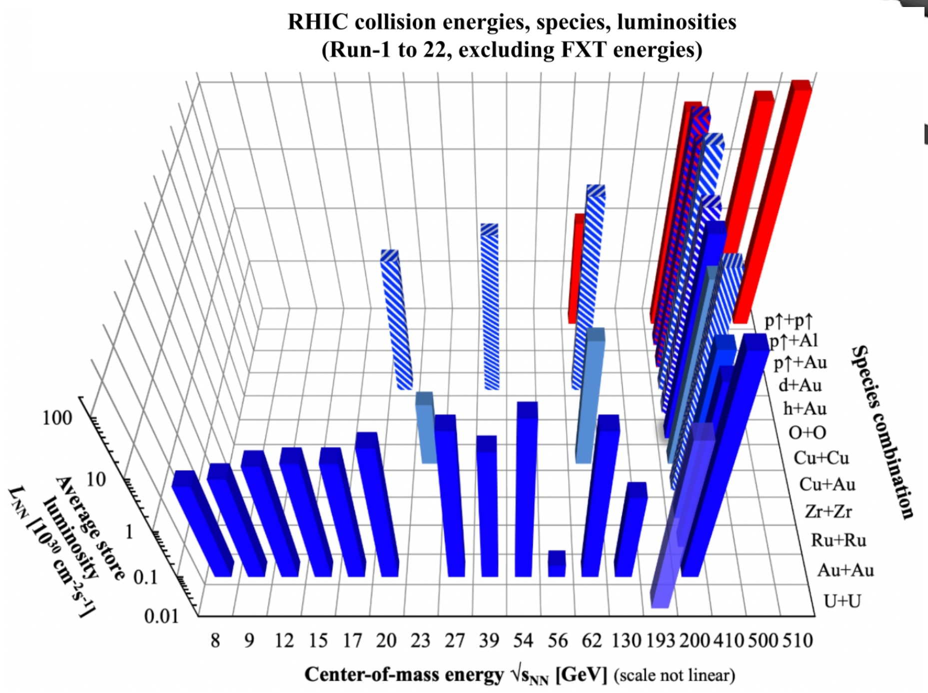

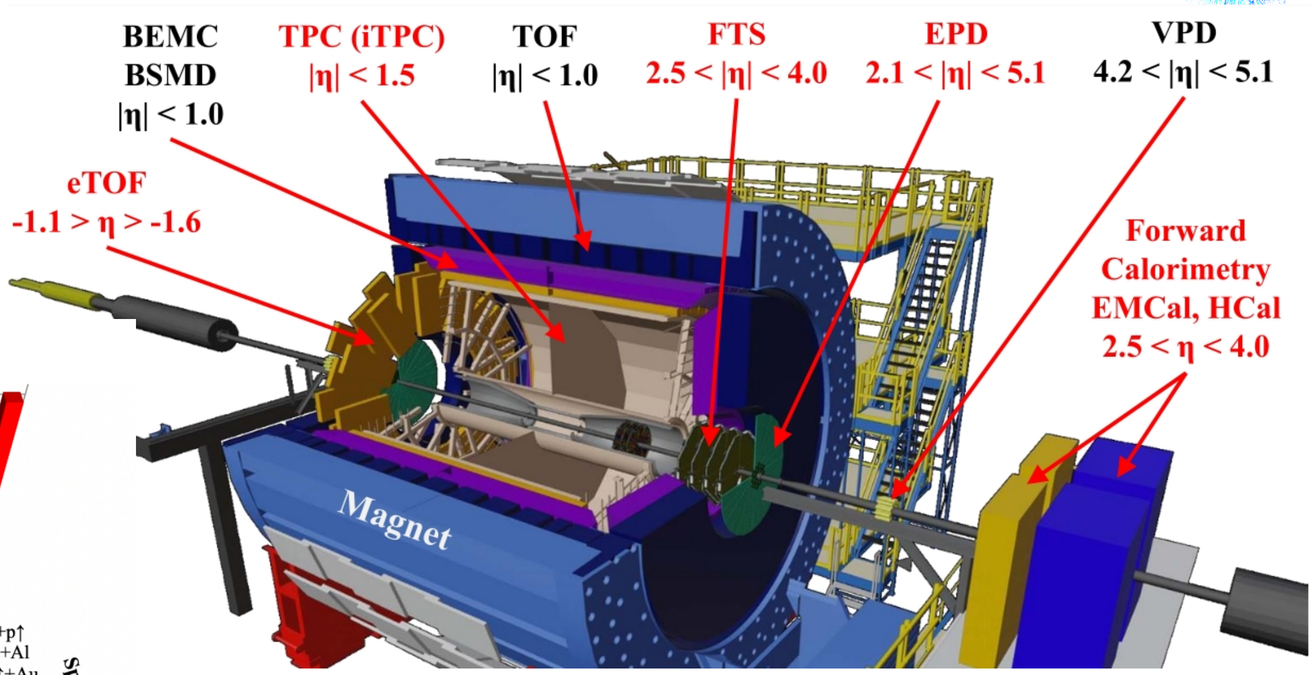

- **BES-II upgrades**: iTPC, eTOF, EPD
- Forward upgrades (2022+):

  Tracking: FTS, Forward Calorimetry: EMCal, HCal

BES-II and Fixed-Target program

➔ Explore QCD phase diagram at finite μ_B

Data taking for BES-II completed

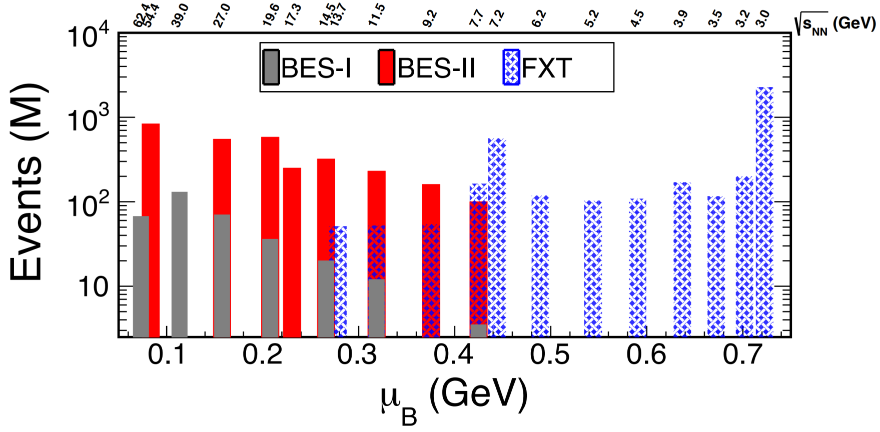

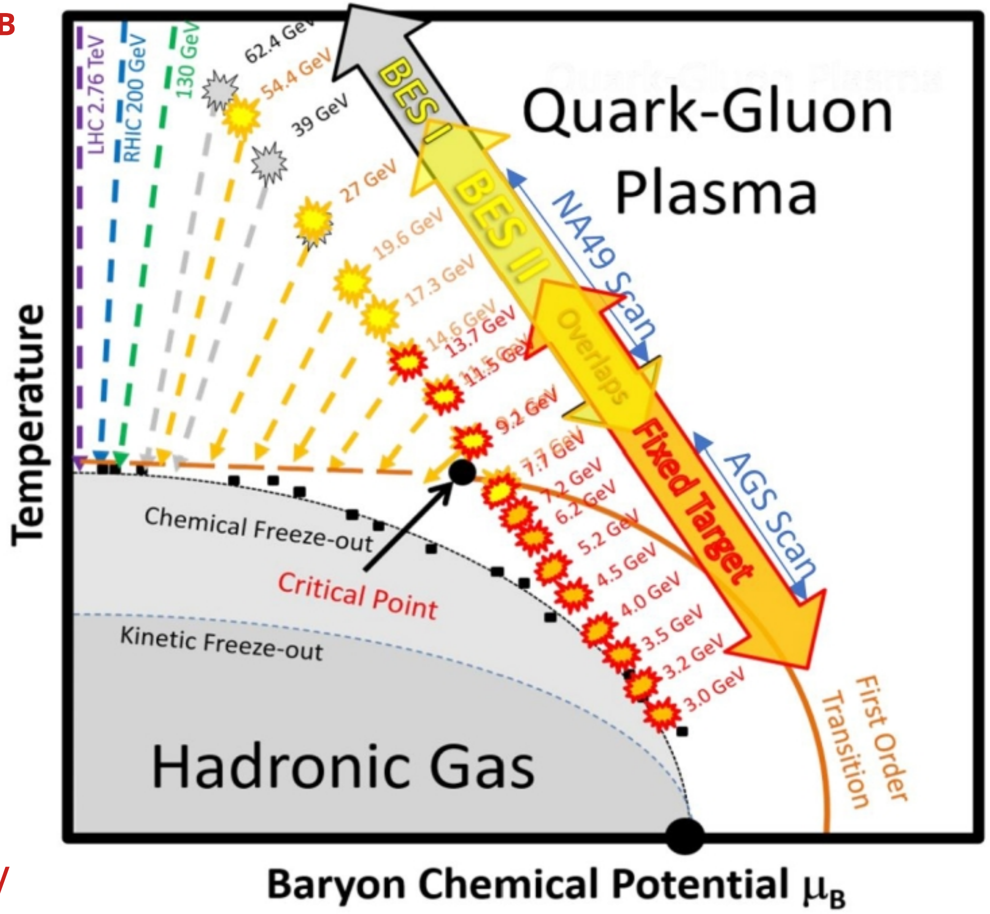

- ➔ Higher statistics than BES-I
- ➔ Wider pseudo-rapidity acceptance
- ➔ Systematically explore high baryon density region (200 < μ_B < 750 MeV)
- ➔ Fixed target program extends μ_B reach to 750 MeV

BES-II and Fixed-Target setup

➔ Explore QCD phase diagram at finite μ_B

Data taking for BES-II completed

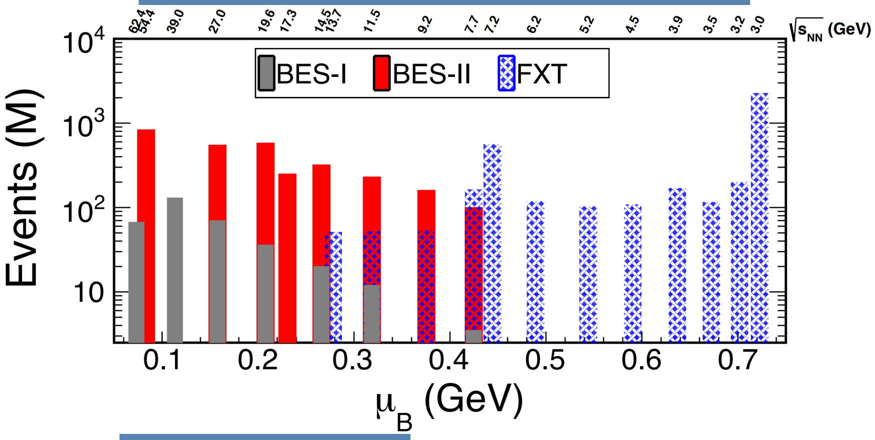

BES-II Upgrades

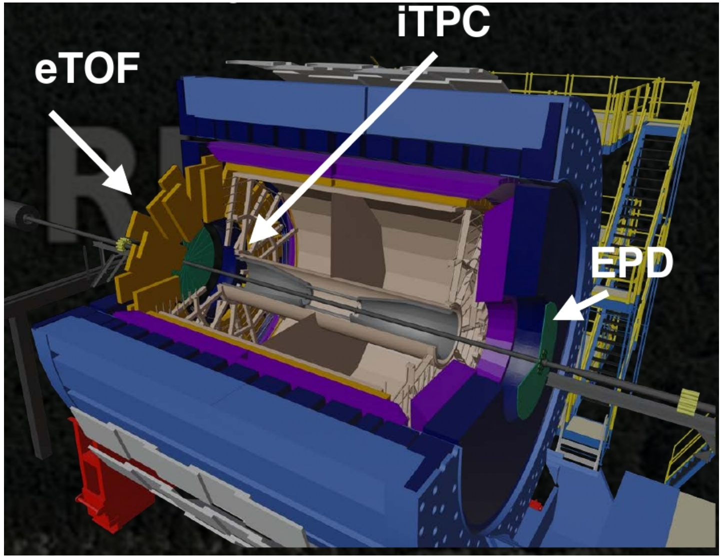

- ➔ **iTPC (2019+)**
  - Extended η acceptance and improved tracking and dE/dx resolution
- ➔ **eTOF (2019+)**
  - Extended PID in forward region
- ➔ **EPD (2018+)**
  - Improved EP resolution, centrality detector

Fixed Target

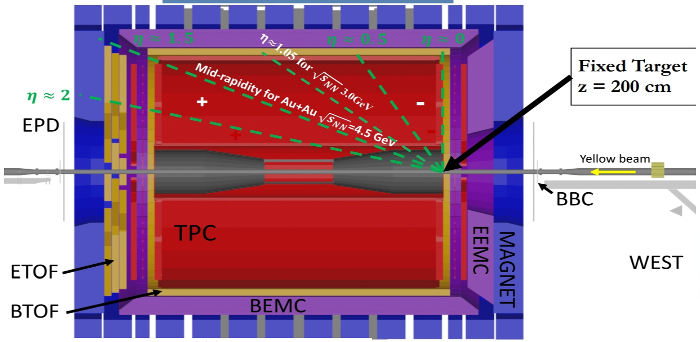

In C.M. frame, $y_{target} = -1.045$ for the 3GeV collisions

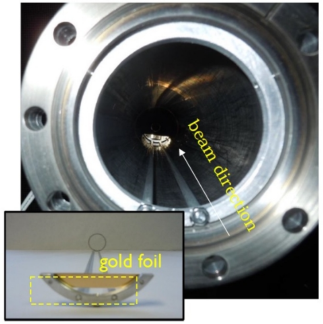

Full Coverage from y=0 to target in 3 GeV Au+Au

Search for CP: net-proton cumulants

- Cumulants of conserved charge distributions relate to correlation length in the medium
- C_4/C_2: non-monotonic behaviour expected around critical point
  - n: net-proton multiplicity in an event $\delta n = n - \langle n \rangle;\ C_2 = \langle \delta n^2 \rangle;\ C_4 = \langle \delta n^4 \rangle - 3\langle \delta n^2 \rangle$

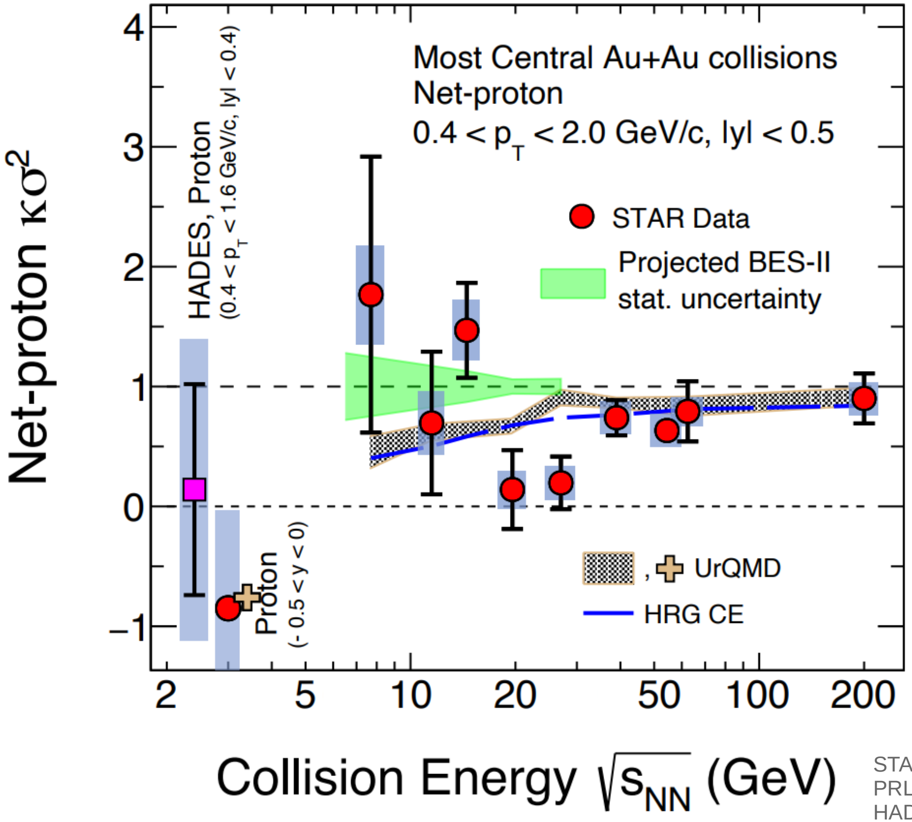

➔ **Hint of non-monotonic trend in BES-I**

➔ Solid conclusion require confirmation from precision measurements with BES-II data

STAR: PRL 127, 262301 (2021), PRC 104, 24902 (2021);
PRL 128, 202302 (2022), PRC 107, 24908 (2023)
HADES: PRC 102, 024914 (2020)

Search for CP: net-proton cumulants

- Cumulants of conserved charge distributions relate to correlation length in the medium
- C_4/C_2: non-monotonic behaviour expected around critical point

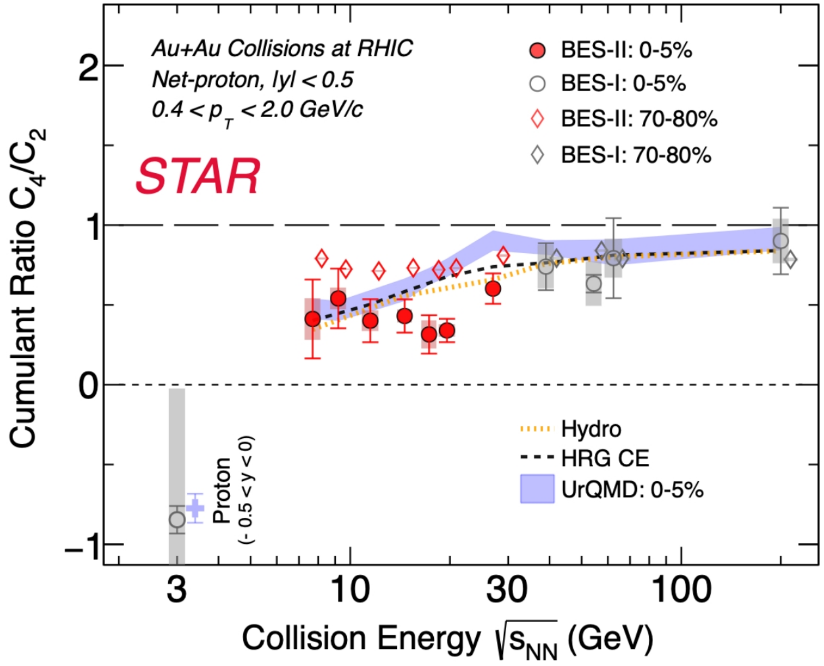

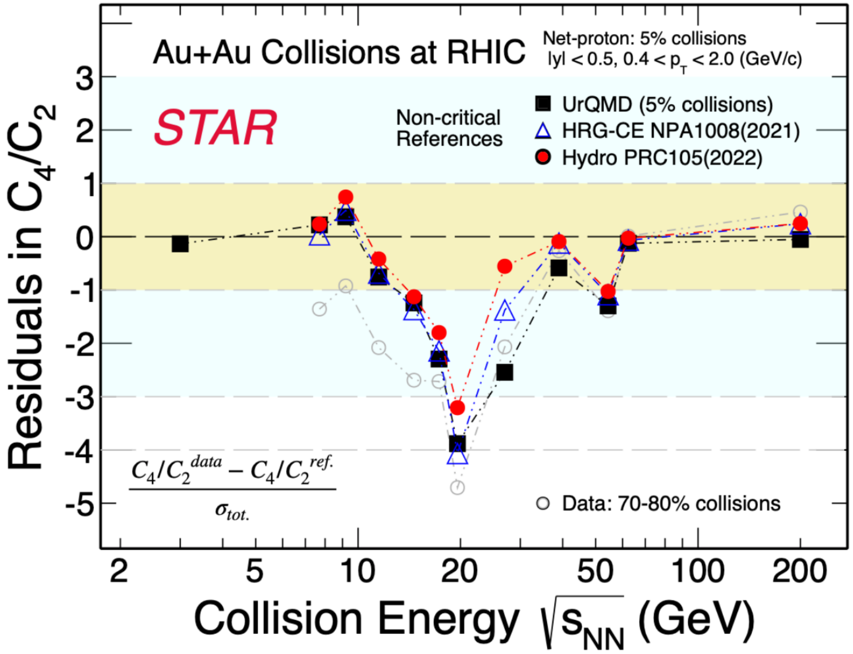

➔ New high-precision BES-II measurement for $\sqrt{s_{NN}}$ = 7.7-27 GeV

➔ C_4/C_2 shows minimum at ~20 GeV compared to 70-80% data and models without CP

Elliptic flow at BES-II

- Equation of State of the medium; constituent interactions and degrees of freedom
- Number of Constituent Quark Scaling: Each quark flows independently
  - Expected universal curve for v_2 vs m_T per quark

Initial spatial anisotropy →
Pressure gradient →
Momentum space anisotropy

$$E\frac{d^3N}{dp^3} = \frac{1}{2\pi}\frac{d^2N}{p_T dp_T dy}\left(1 + \sum 2v_n \cos n(\phi - \Psi_n^{EP})\right)$$

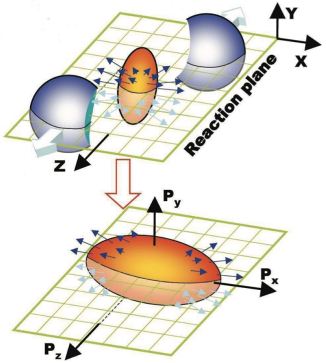

$$v_1 = \langle\frac{p_x}{p_T}\rangle$$

$$v_2 = \langle\frac{p_x^2 - p_y^2}{p_x^2 + p_y^2}\rangle$$

v_2 reflect asymmetry on X-Y plane

Elliptic flow at BES-II

- Equation of State of the medium; constituent interactions and degrees of freedom
- Number of Constituent Quark Scaling: Each quark flows independently
  - **Universal curve for v_2 vs m_T per quark at $\sqrt{s_{NN}}$ > 7.7 GeV**

STAR Collaboration, Phys. Rev. Lett. 110, 142301 (2013)
Phys. Rev. C 93, 14907 (2016), Phys. Lett. B 827, 137003 (2022)

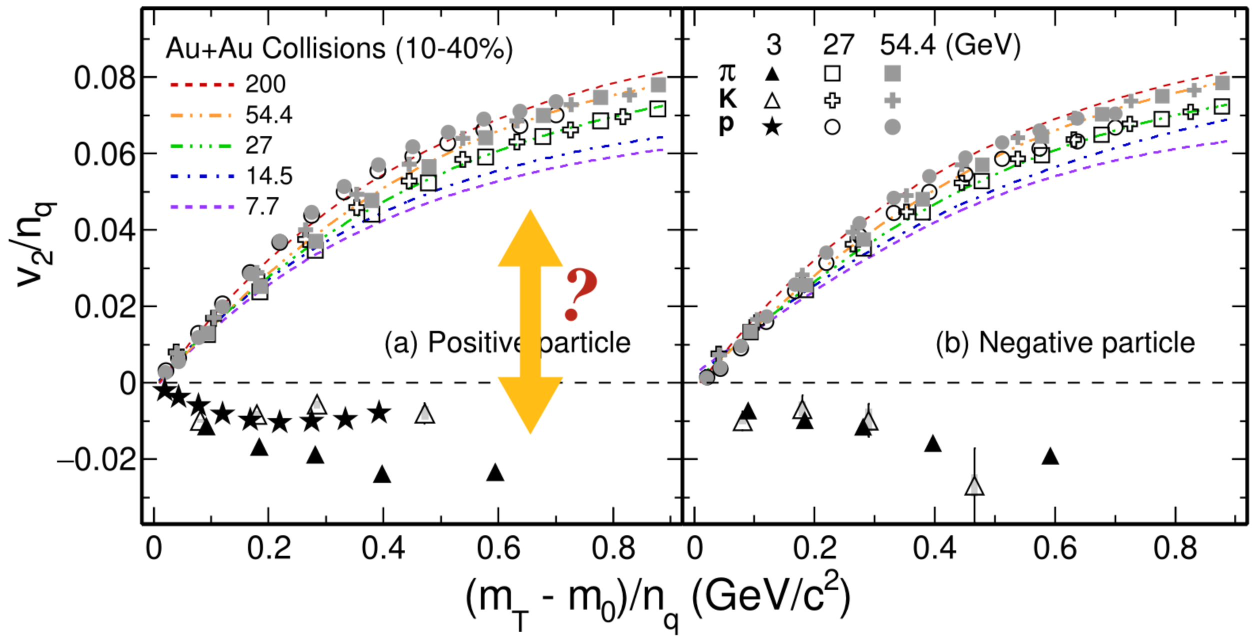

Initial spatial anisotropy →
Pressure gradient →
Momentum space anisotropy

$$E\frac{d^3N}{dp^3} = \frac{1}{2\pi}\frac{d^2N}{p_T dp_T dy}\left(1 + \sum 2v_n \cos n(\phi - \Psi_n^{EP})\right)$$

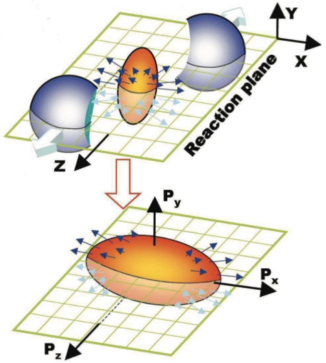

$$v_2 = \langle \frac{p_x^2 - p_y^2}{p_x^2 + p_y^2} \rangle$$

₂ reflect asymmetry on X-Y plane

➔ Partonic collectivity at $\sqrt{s_{NN}}$ = 7.7 – 200 GeV; $\sqrt{s_{NN}}$ = 3 GeV: hadronic interactions dominate

➔ Change of degrees of freedom 3 – 7.7 GeV ?

Elliptic flow at high high μ_B region

- Light and strange hadron elliptic flow

Hadronic interaction ← Collision energy

Partonic interaction Collision energy →

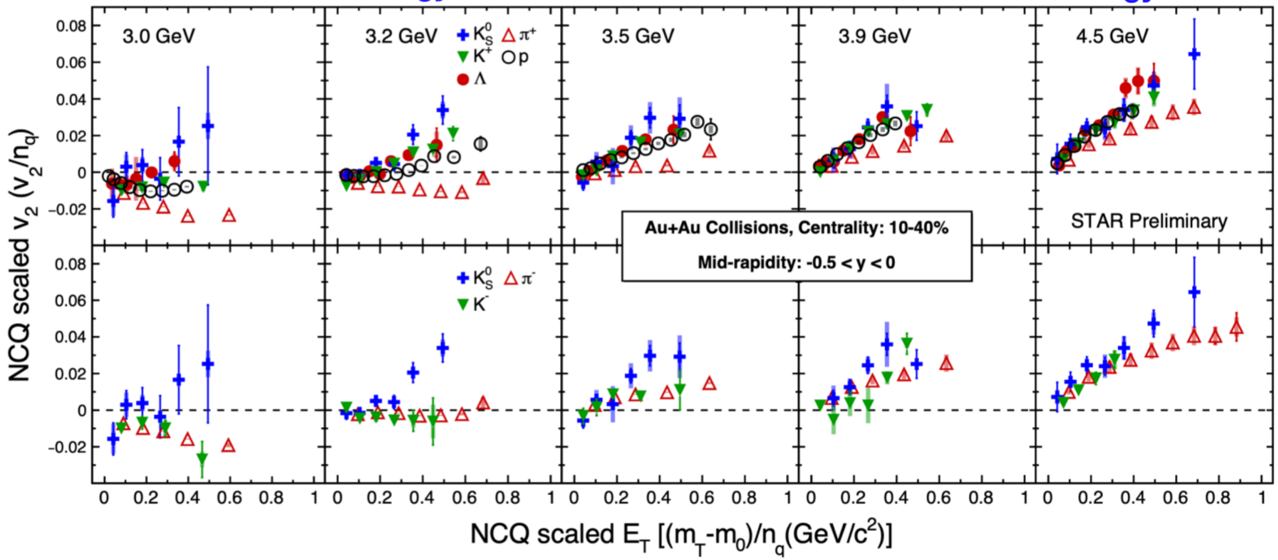

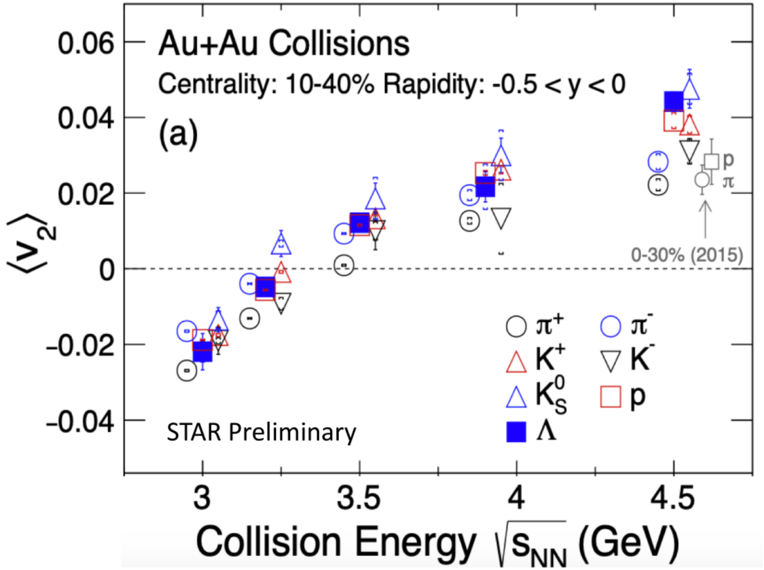

➔ v_2 NCQ scaling breaks at $\sqrt{s_{NN}}$ = 3.2 GeV and below, gradually restores towards 4.5 GeV

➔ **Dominance of hadronic matter at the high-baryon-density region**

➔ **Negative → positive v_2: Out-of-plane → In-plane expansion** between 3 - 4.5 GeV

Energy dependence of v_1 slope at high μ_B

- Sensitive probe of the Equation of State of the dense matter

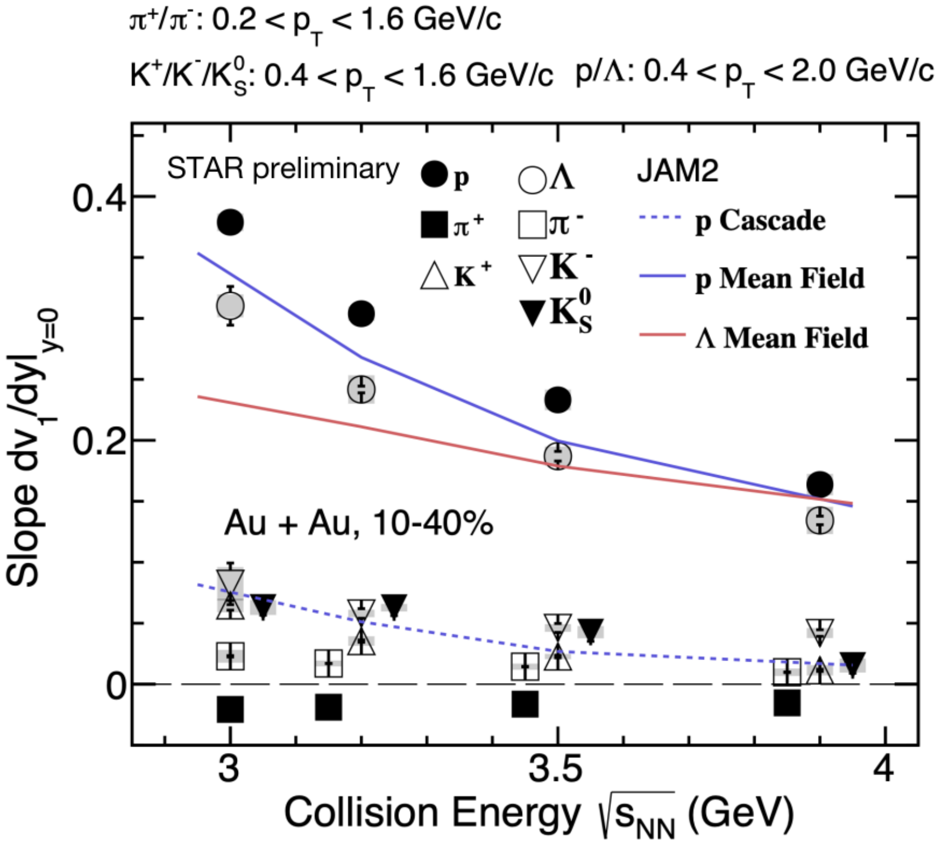

- ➔ π, K, p, Λ measured across collision energies at high μ_B
- ➔ Positive v_1 slope; v_1 slope of baryons drops as collision energy increases
- ➔ Hadronic transport model JAM2 with baryonic mean-field interactions better describe data
  - ➔ EoS dominated by baryonic interactions at high μ_B

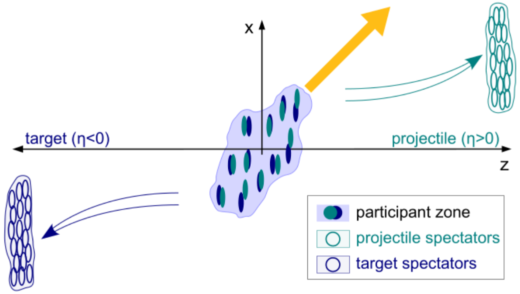

$$v_1 = \langle \frac{p_x}{p_T} \rangle$$

v_1 reflect asymmetry along *x* direction

Figure: Phys. Rev. Lett. 111, 232302 (2013)

Strangeness production at high μ_B

- Sensitivity to nuclear Equation of State
- Comprehensive measurements of strange hadron production at FXT energies

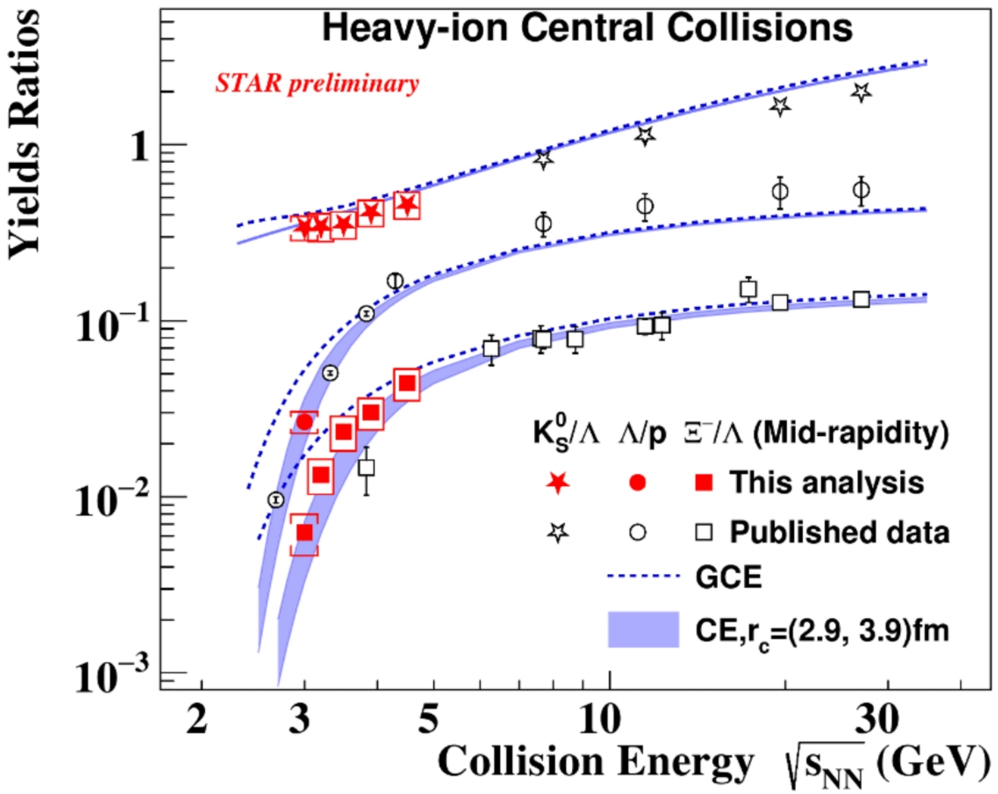

➔ Grand Canonical Ensemble (GCE) fails for $\sqrt{s_{NN}}$ < 4 GeV;

  ➔ Local strangeness conservation required – **Canonical Ensemble favored**, with strangeness correlation length 2.9 - 3.9 fm

➔ **Change of medium properties at the high-baryon-density region**

Global Λ polarization

- Vorticity of the medium and magnetic field

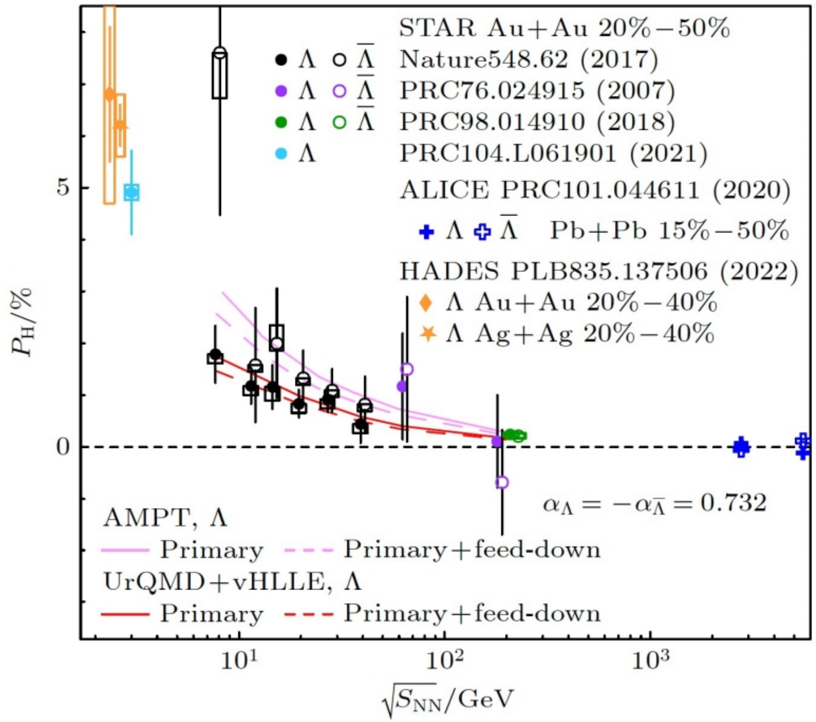

Acta Phys. Sin. Vol. 72, No. 7(2023) 072401

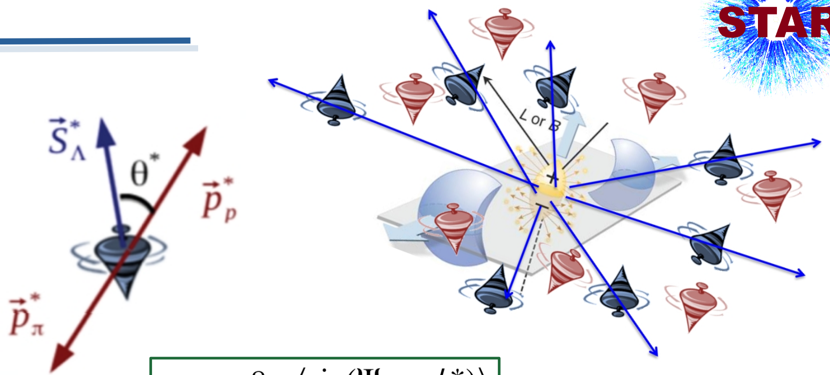

$$P_H = \frac{8}{\pi \alpha_H} \frac{\langle \sin(\Psi_1 - \phi_d^*) \rangle}{\mathrm{Res}(\Psi_1)}$$

Fluid vorticity → Λ, anti-Λ in same direction

$$\omega = k_B T (P_\Lambda + P_{\bar{\Lambda}})/\hbar$$

Magnetic field → Λ, anti-Λ in opposite direction

$$B = \frac{T}{2\mu_\Lambda}(P_\Lambda - P_{\bar{\Lambda}})$$

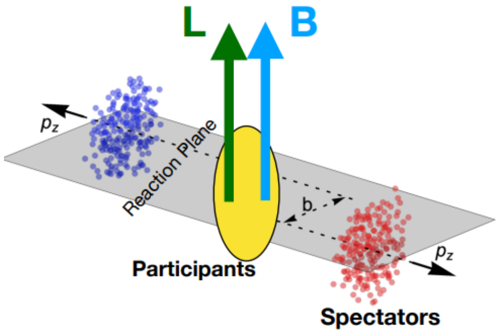

➔ **Increasing global polarization, P_H, trend down to $\sqrt{s_{NN}}$ = 3 GeV**

➔ **Difference between Λ and anti-Λ ?**

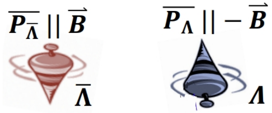

Energy dependence of Λ polarization

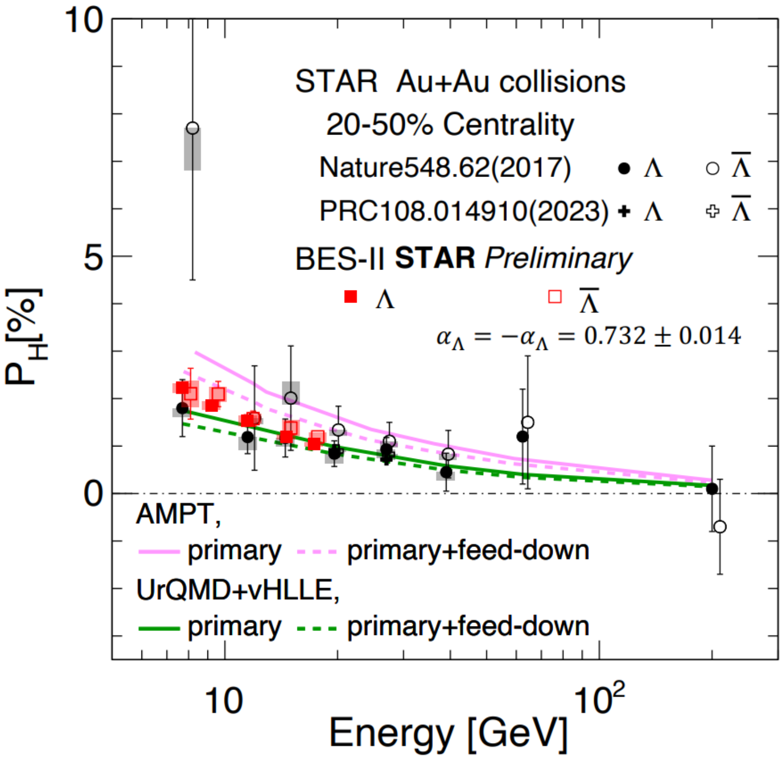

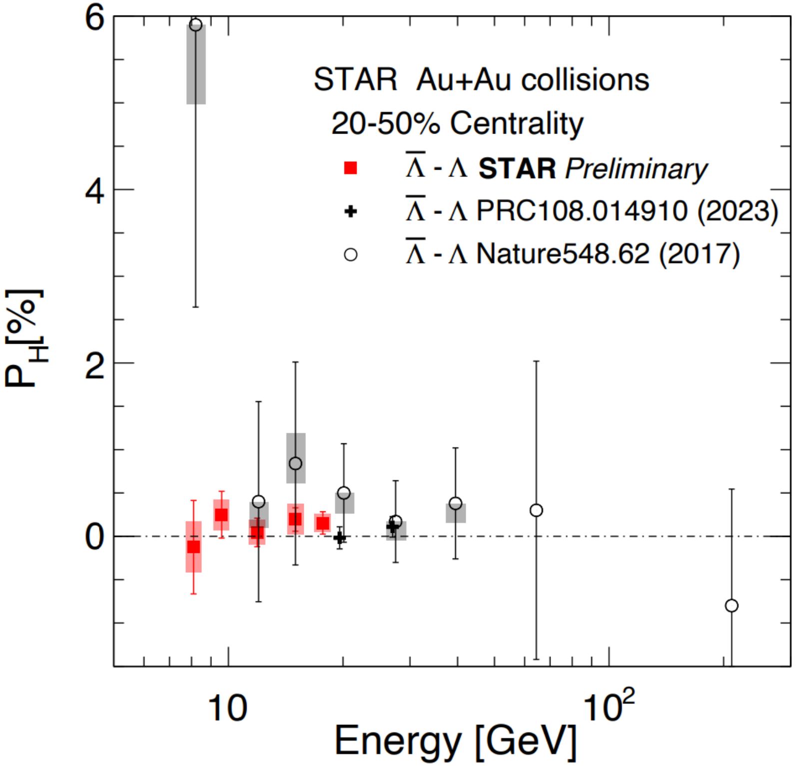

- New STAR preliminary results at $\sqrt{s_{NN}}$ =7.7-17.3 GeV from BES-II: significant improvement in precision
- No splitting between Λ and anti-Λ global polarization within uncertainties
  - Upper limit on late stage magnetic field

- 95% confidence level STAR, PRC 108,014910(2023)
- $B < 9.4\times10^{12}\ T$ at 19.6 GeV
- $B < 1.4\times10^{13}\ T$ at 27 GeV

Thermal dielectron spectra

- Direct access to temperature of QGP phase and partonic → hadron phase transition

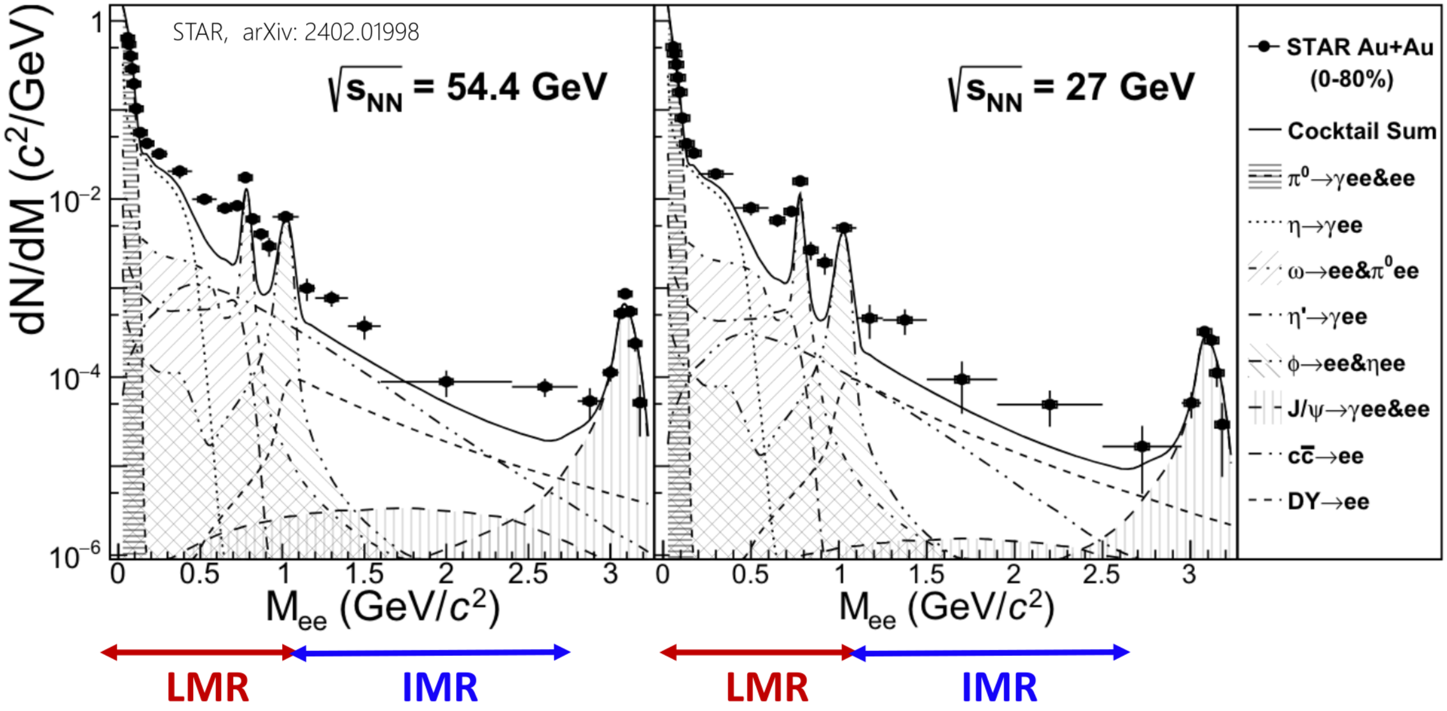

➔ Clear enhancement compared to hadronic cocktail in both low mass region (LMR) and intermediate mass region (IMR)

Thermal dielectrons vs μ_B

- Direct access to temperature of QGP phase and partonic → hadron phase transition

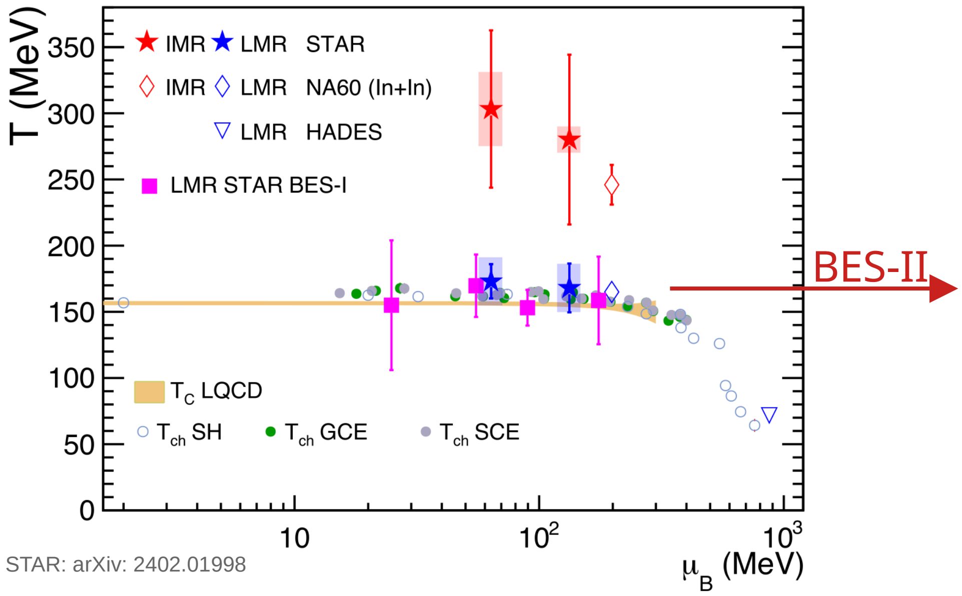

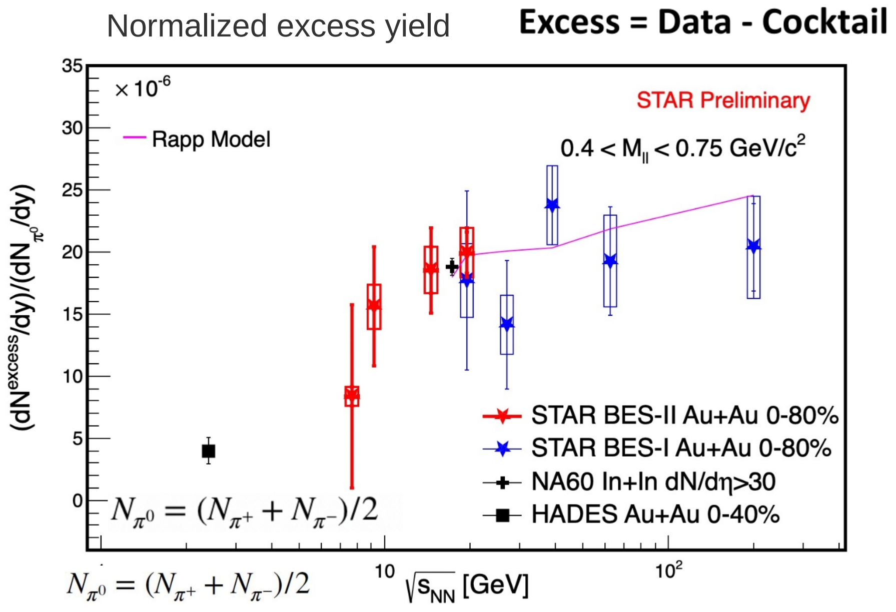

- ➔ T^{LMR} is close to both T_{ch} and T_{pc} → Emitted from hadronic phase
- ➔ T^{IMR} is higher than T^{LMR} → Emitted from partonic QGP phase

- ➔ The integrated excess yield (data - cocktail, normalized by $N\pi^0$) shows a hint of decreasing trend with increasing μ_B
- ➔ Connection between STAR BES-I and HADES data

Energy dependence of J/ψ production

- Medium thermodynamic properties

Dissociation

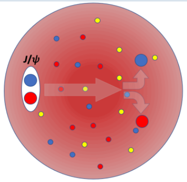

Regeneration

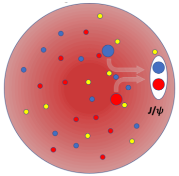

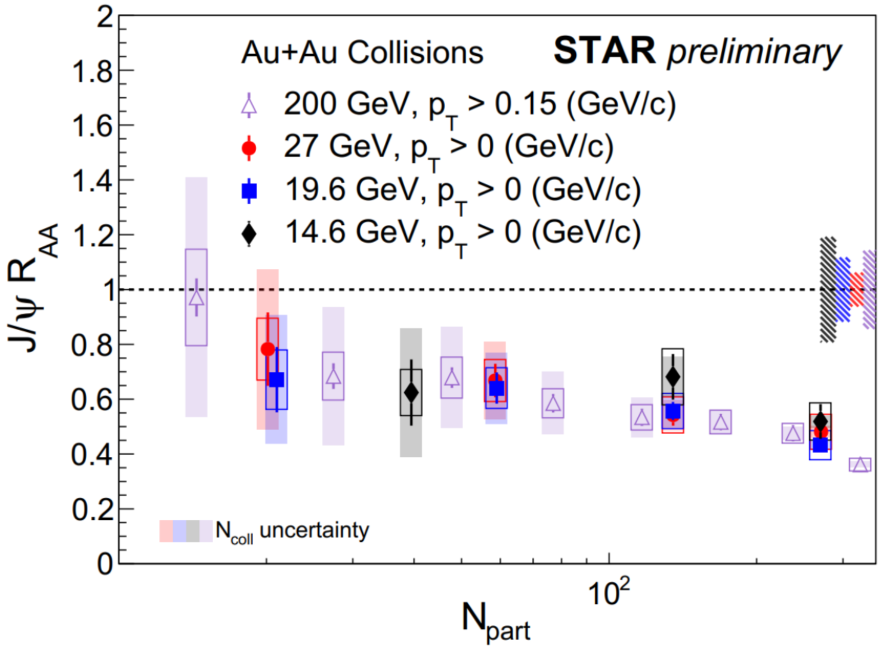

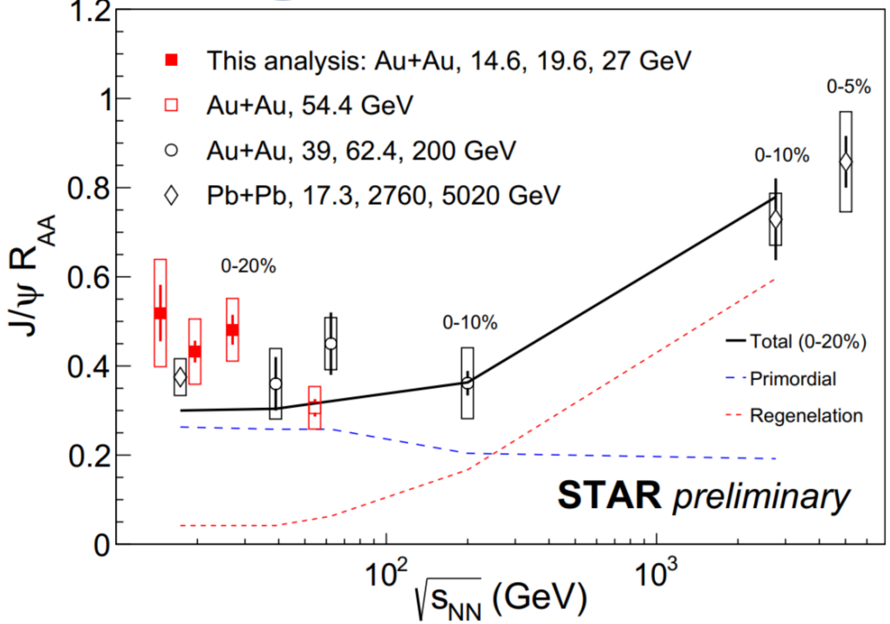

X. Zhao, R. Rapp, Phys. Rev. C 82 (2010) 064905 (private communication).
L. Kluberg, Eur. Phys. J. C 43 (2005) 145.
NA50 Collaboration, Phys. Lett. B 477 (2000) 28

- ➔ No significant energy dependence of the J/ψ suppression at RHIC at similar N_{part}
- ➔ Central collisions: no significant energy dependence from $\sqrt{s_{NN}}$ = 7.7 up to 200 GeV
  - ➔ Interplay of dissociated and regeneration effects from RHIC to LHC energies

Sequential suppression of quarkonia

- Medium thermodynamic properties

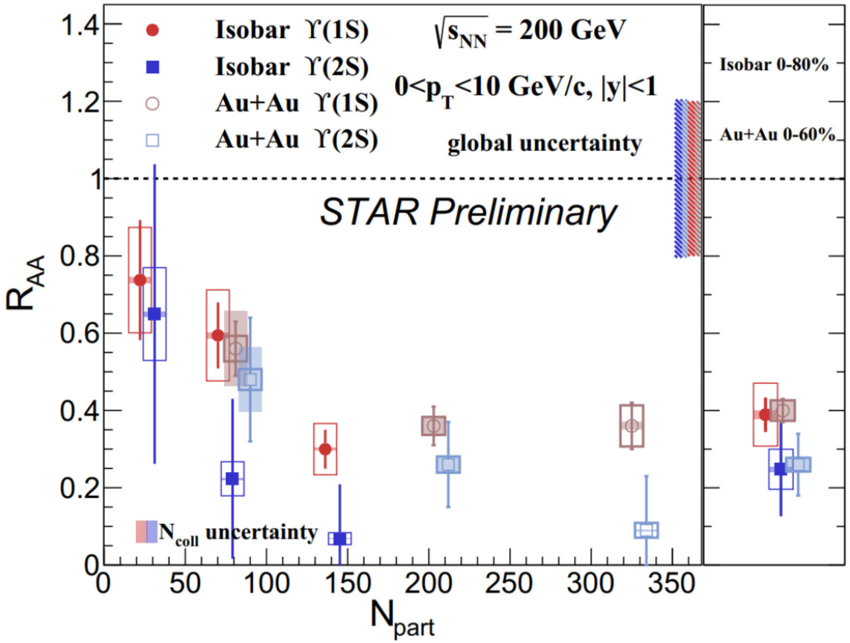

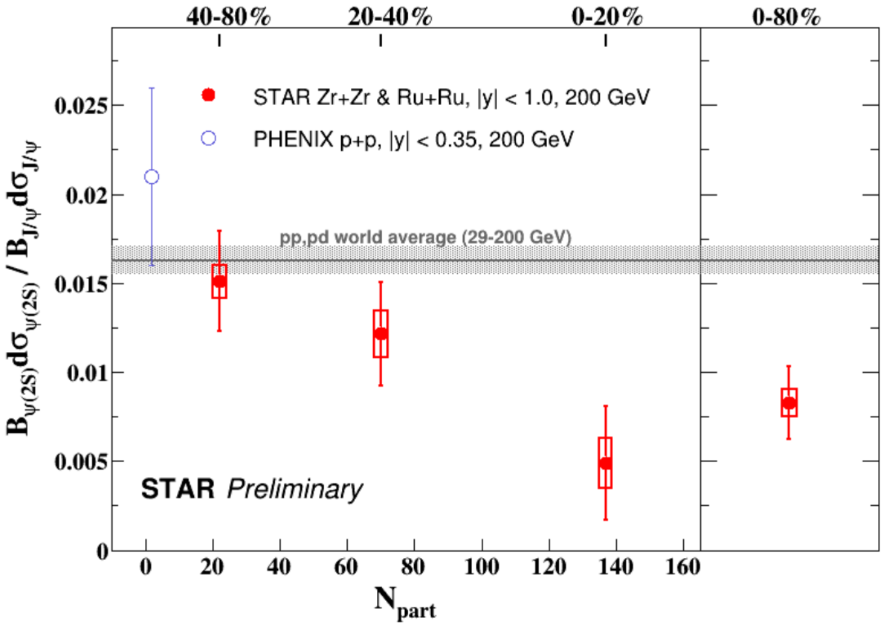

➔ Hint of sequential Upsilon suppression in isobar collisions, similar to that in Au+Au at similar <N_{part}>

➔ First observation of charmonium sequential suppression in heavy-ion collisions at RHIC

Hypernuclei production in HI collisions

- **Production mechanism of hypernuclei is still not well understood**
- Natural laboratory to study **Hyperon-Nucleon (Y-N) interactions** → EOS of neutron stars

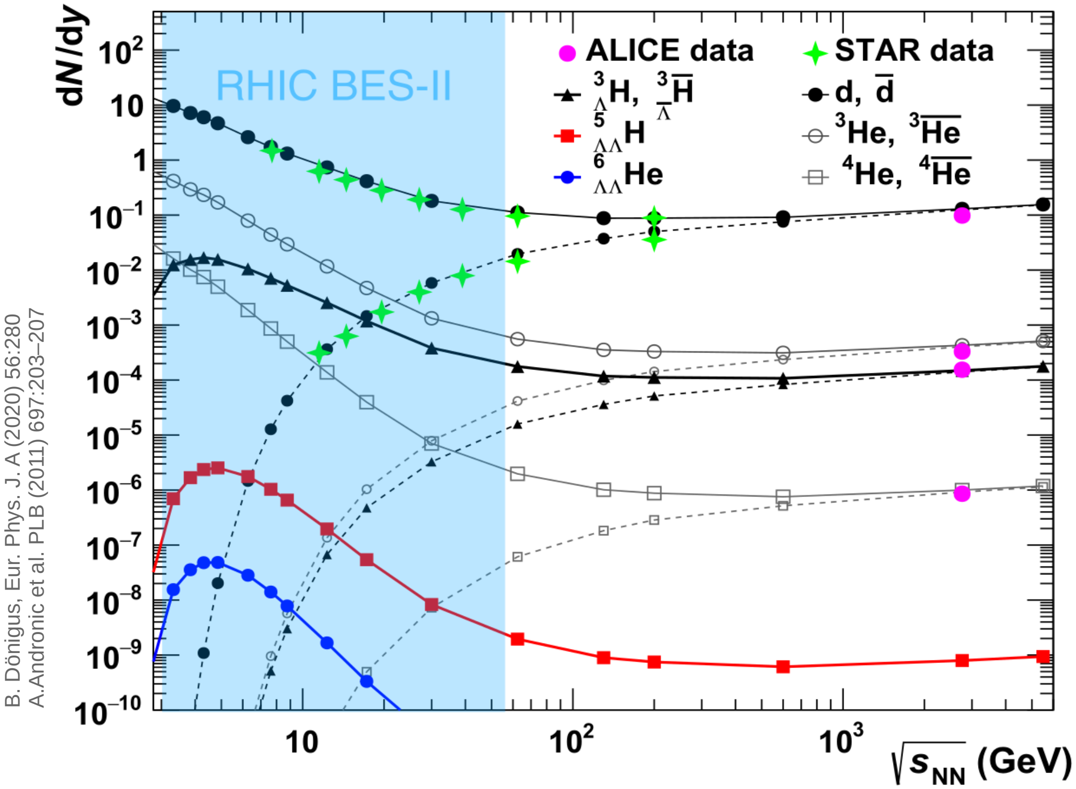

➔ High baryon density → enhanced production of hypernuclei

➔ RHIC BES-II offers great opportunity for hypernuclei measurements.

Hypernuclei production and lifetime

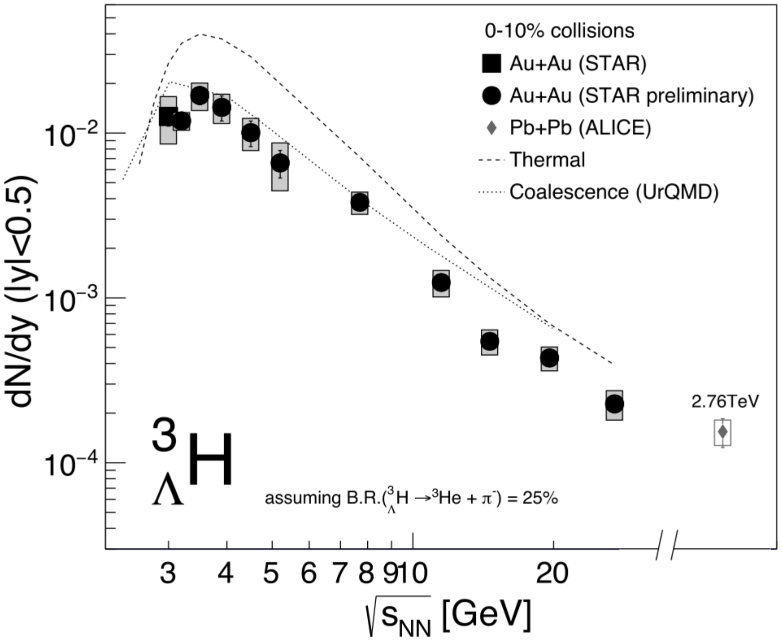

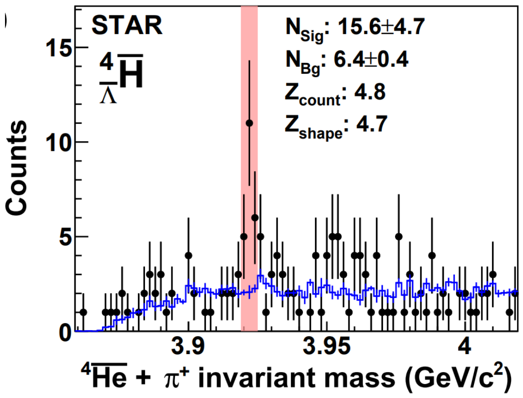

STAR,Nature 2024 (2024) 77

STAR, PRL 128 (2022) 202301
ALICE, PLB 754 (2016) 360
T. Reichert, et al, PRC 107 (2023) 014912

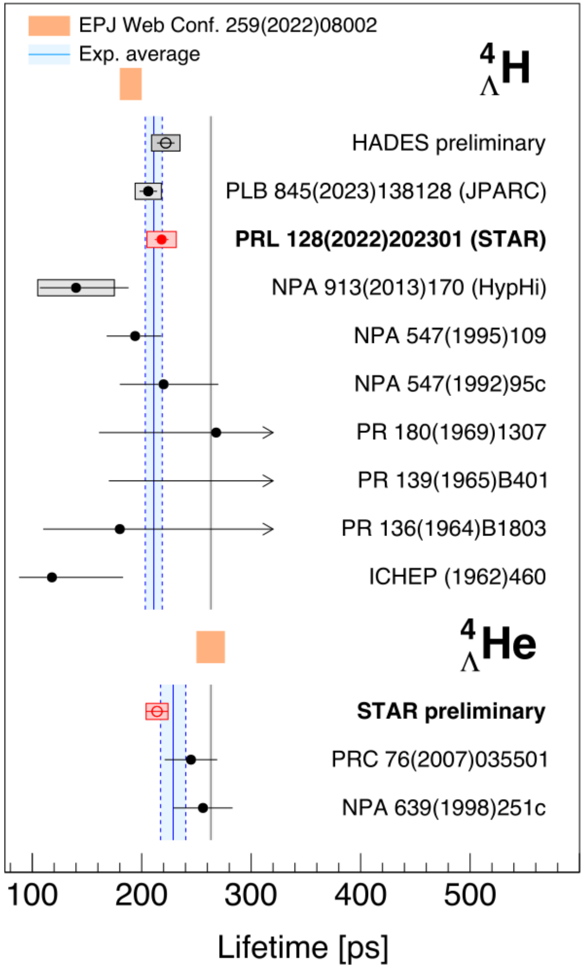

- **First energy dependence of $^{3}_{\Lambda}H$ production yields in high-μ_B region**
  - Hadronic transport + coalescence models qualitatively describe the data
- The first observation of **Anti-Hyper-Hydrogen-4**
- Precise **$^{4}_{\Lambda}H$ and $^{4}_{\Lambda}He$ lifetimes** measurements in heavy-ion collisions
- Towards quantitative understanding of Y-N interaction

Hypernuclei <p_T> at high μ_B

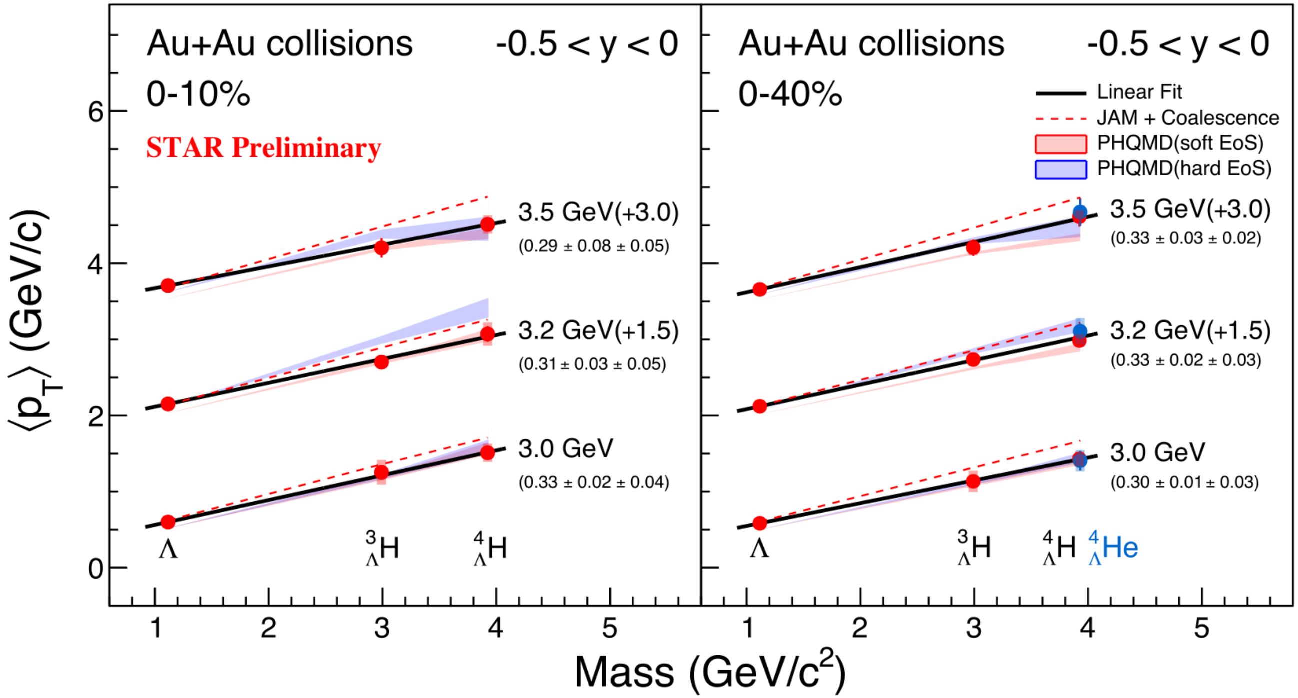

- ➔ $\langle p_T \rangle$ vs mass follows a linear mass scaling at $\sqrt{s_{NN}}$ = 3.0, 3.2, 3.5 GeV
- ➔ Particle yields + <p_T> slope + v_1 slope (backup) support coalescence picture of hypernuclei production at mid-rapidity

Light (hyper-)Nuclei-to-Hadron ratios

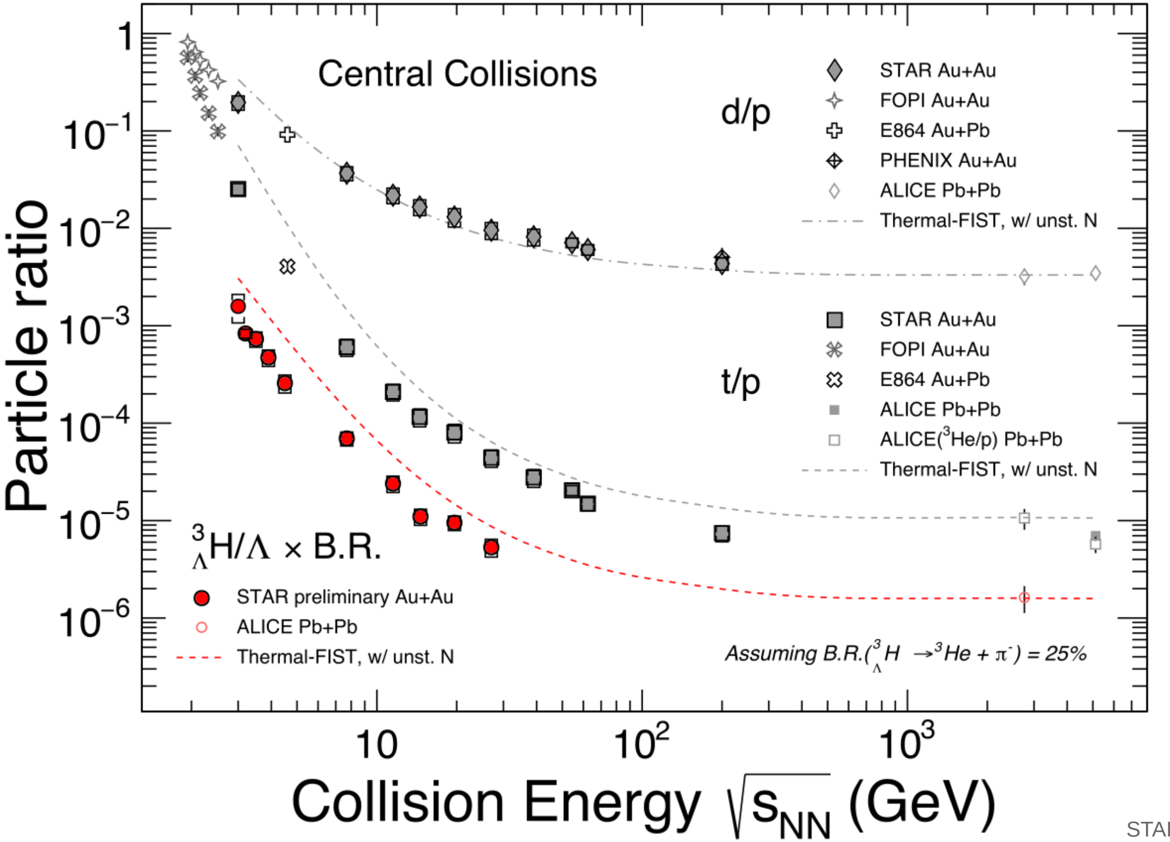

- ➔ Thermal model overpredicts t/p and $^{3}_{\Lambda}H$ /Λ ratios
- ➔ Suggests that $^{3}_{\Lambda}H$ and t yields are not in equilibrium and fixed at chemical freeze-out simultaneously with other hadrons

STAR, PRL 130 (2023) 202301
STAR, arXiv: 2311.11020
T. Reichert, et al, PRC 107 (2023) 014912

Baryon number carrier

- Central collisions, $B \times \Delta Z/A \sim 2 \times \Delta Q$
  - significantly higher than naïve expectation of 1 for valence quarks carrying baryon number

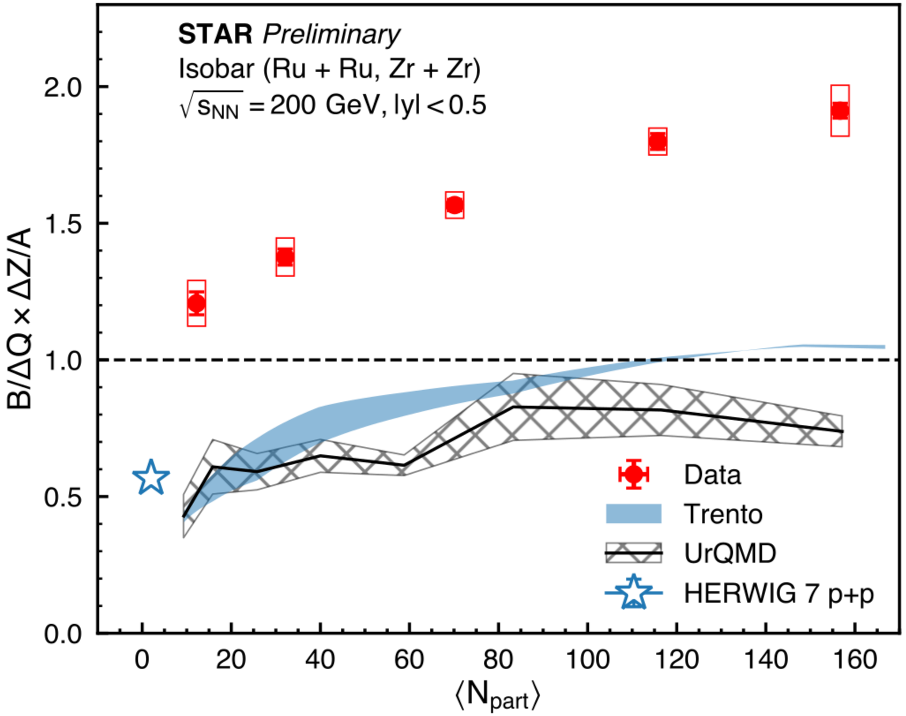

Valence Quarks vs. **Junctions**

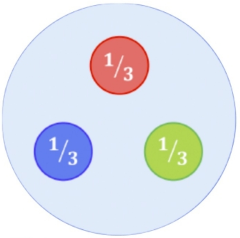

VS.

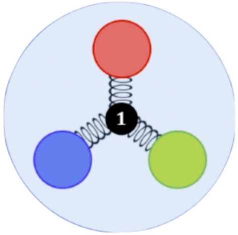

X. Artru, Nucl. Phys. B 85 (1975) 442
G. C. Rossi, G. Veneziano, Nucl. Phys. B 123 (1977) 507

Valence Quarks:
- Carry large momentum fractions
- Hard to be stopped at midrapidity

Junctions:
- Consist of low-momentum gluons
- Easier to be stopped at midrapidity

Valence Quarks:
- $Q \sim B \times Z/A$

Junctions:
- $Q < B \times Z/A$

Baryon number carrier

- Central collisions, B×ΔZ/A ~ 2×ΔQ
  - significantly higher than naïve expectation of 1 for valence quarks carrying baryon number

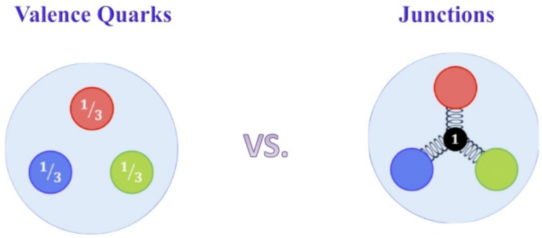

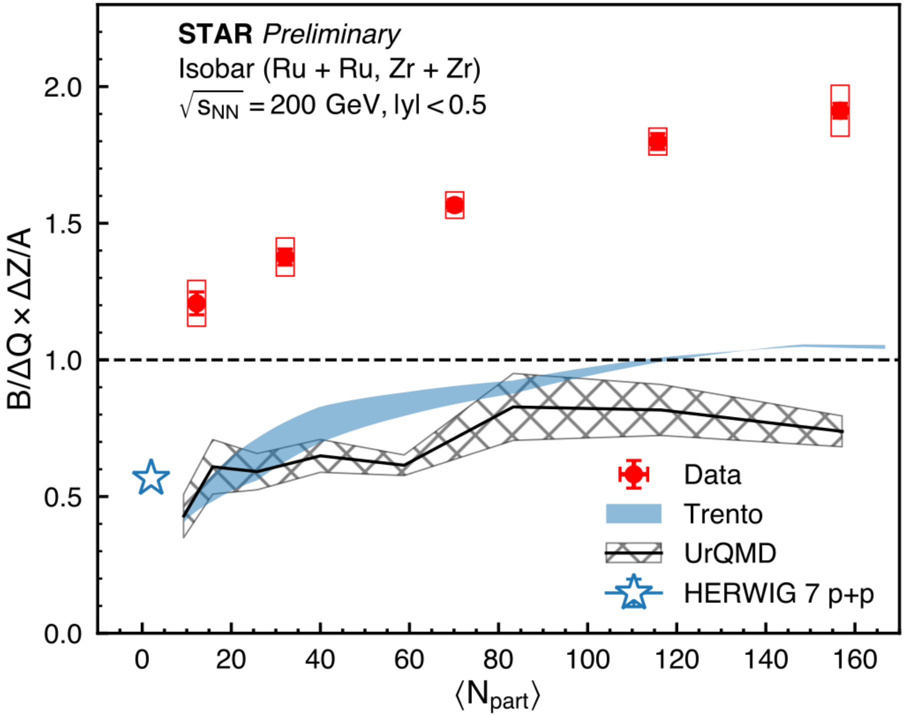

- Three independent experimental tests performed
  - Isobar collisions: significantly more baryon transport than charge transport
  - γ+Au: clear baryon transport with a rapidity slope smaller than PYTHIA predictions
  - Au+Au: rapidity slope independent of centrality
- All disfavour the scenario where the baryon number is carried by valence quarks

Strangeness production at high energy

- Strangeness production dependence on the colliding system
- d+Au: bridge the multiplicity gap between peripheral A+A and *p+p*

Hyperon-to-pion yield ratio

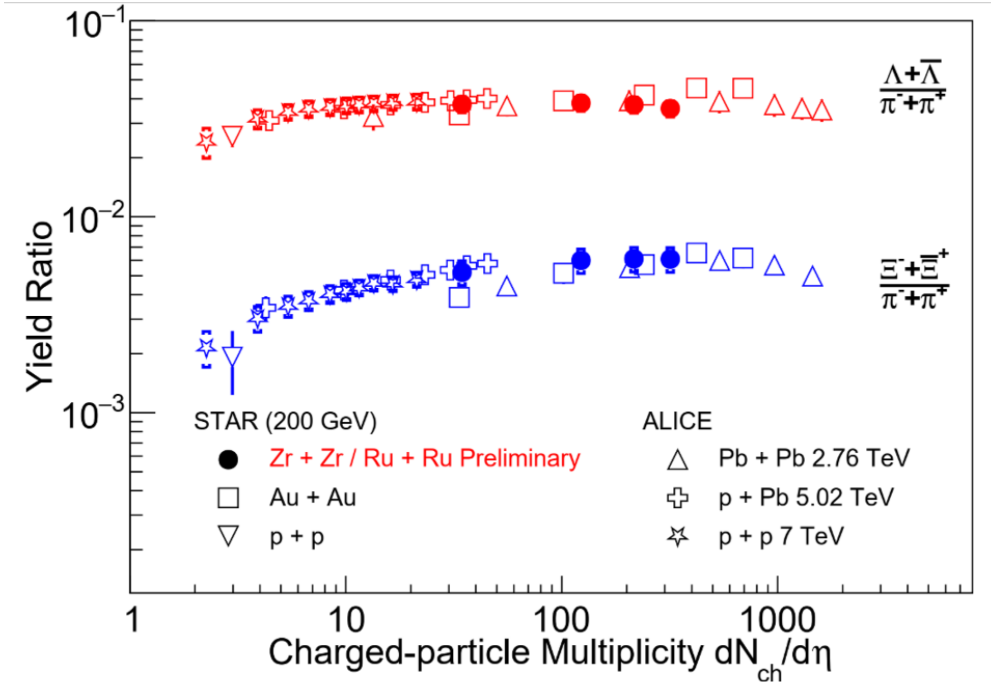

Strange hadron-to-pion yield ratio

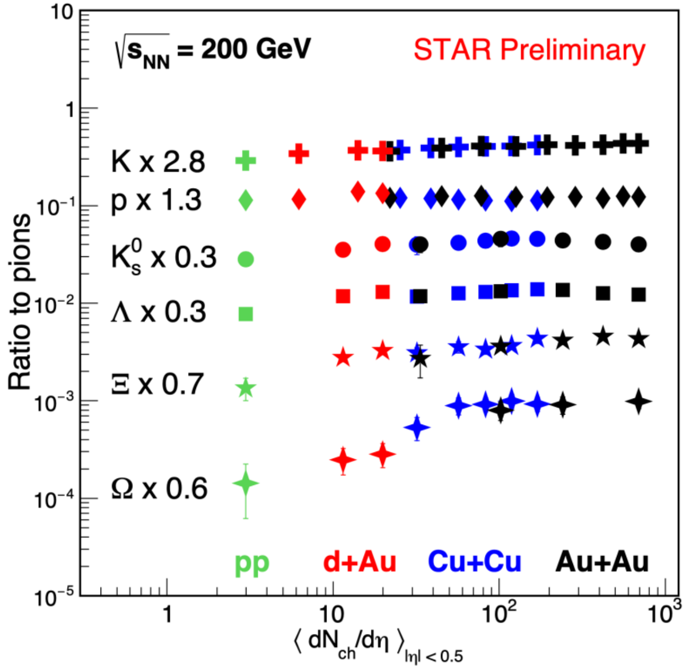

➔ Strangeness production seems to follow a global trend mainly driven by event multiplicity

K^{*0} resonance production in isobar collisions

- Resonance/non-resonance ratio, re-scattering and regeneration effects → probing hadronic phase

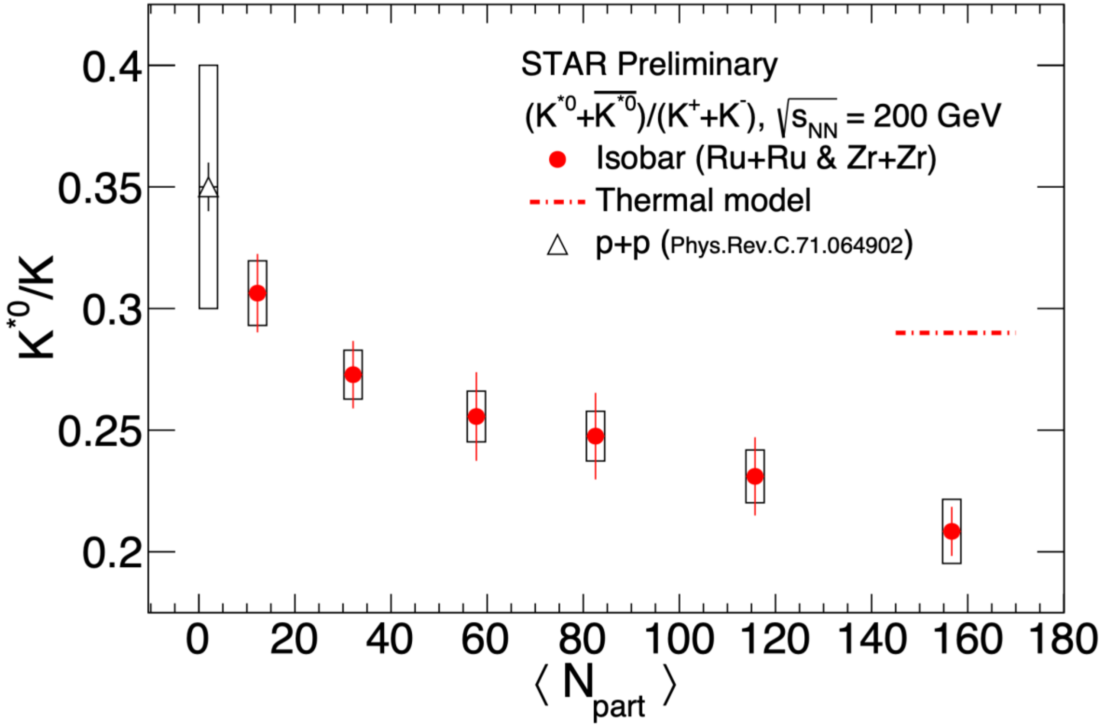

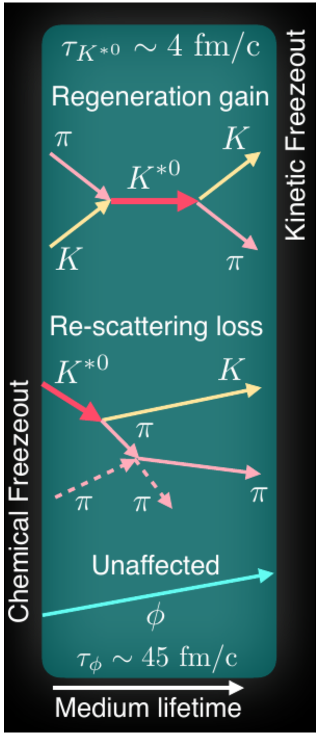

➔ Evidence of late stage hadronic re-scattering effect

Forward Upgrade and 2023-25 Runs

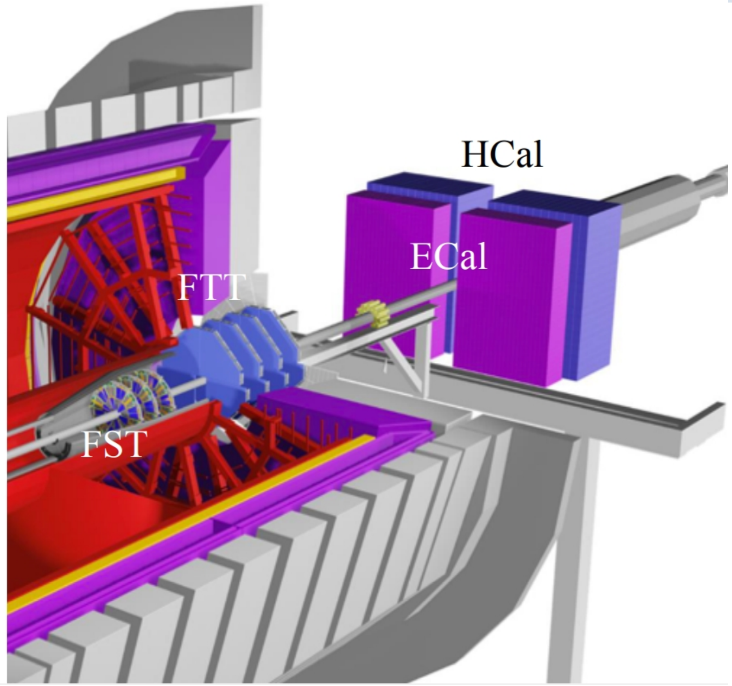

- **Forward Tracking System (FTS)**
  - Forward Silicon Tracker (FST)
  - Forward Small-strip Thin Gap Chambers Tracker (FTT)
- **Forward Colorimeter System (FCS)**
  - Electromagnetic Calorimeter
  - Hadronic Calorimeter

- **Hot QCD – study of microstructure of QGP**

  Au+Au @200 GeV (2023 & 25)
  - What is the nature of the 3-dimensional initial state at RHIC energies?
  - What can be learned about confinement from charmonia measurements?
  - What are the electrical, magnetic and chiral properties of the medium?
  - What is the precise nature of the transition near μ_B=0?

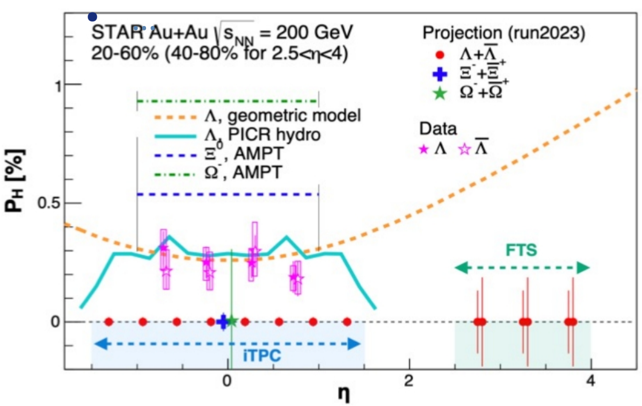

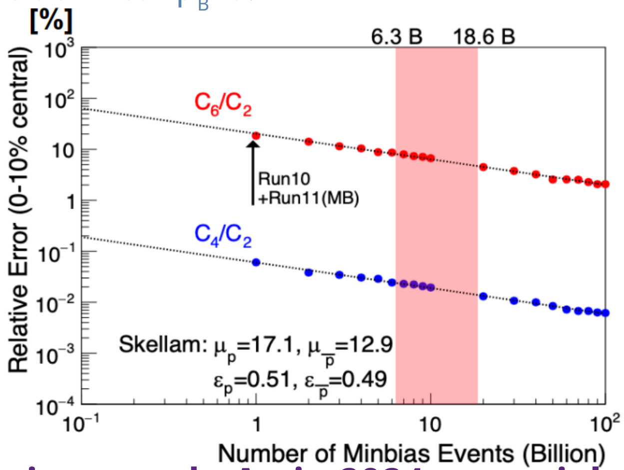

- **Cold QCD: Equal N-N luminosities in pp and pAu in 2024 essential to optimize several critical measurements**
  - First look gluon GPD → Eg
  - Nuclear dependence of PDFs, FF, and TMDs
  - Non-linear effects in QCD

Summary

- Very rich STAR physics program with wide range of colliding species and colliding energies
- Stay tuned for more BES-II and FXT results
- More cold and hot QCD studies with p+p, p+Au and Au+Au @ 200 GeV taken in 2023-2025

Thank you !

Backup

Energy Dependence of C_4/C_2: Comparison with BES-I

- Cumulants of conserved charge distributions relate to correlation length in the medium
- C_4/C_2: non-monotonic behaviour expected around critical point

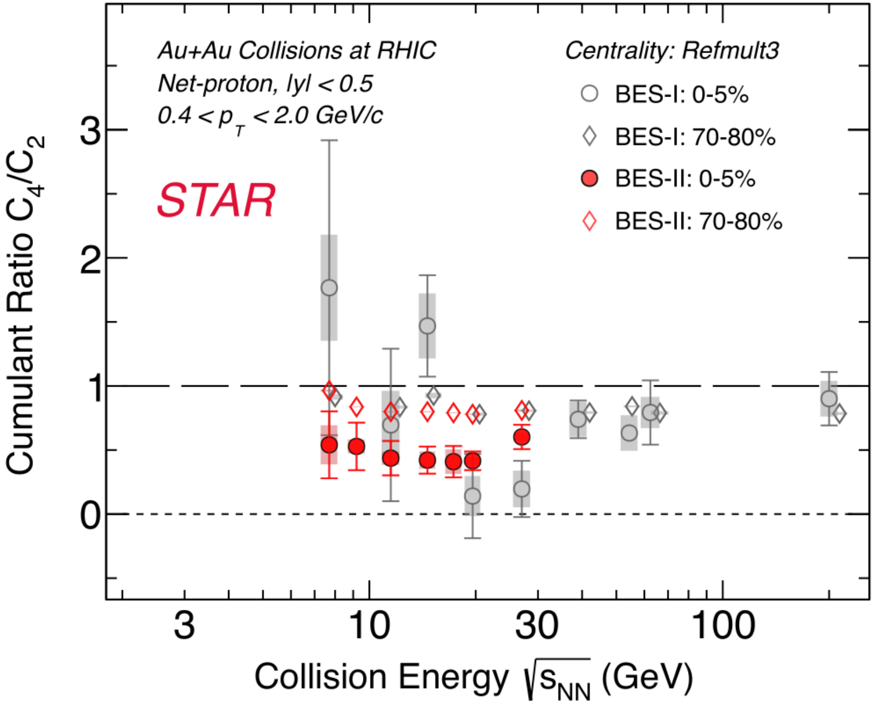

Deviation between BES-II and BES-I data

$\sqrt{s_{NN}}$ (GeV)	0-5%	70-80%
7.7	1.0σ	0.9σ
11.5	0.4σ	1.3σ
14.6	2.2σ	2.5σ
19.6	0.7σ	0.0σ
27	1.4σ	0.2σ

➔ New high-precision BES-II measurement for $\sqrt{s_{NN}}$ = 7.7-27 GeV

➔ BES-II results consistent with BES-I within uncertainties

Anisotropic flow

- Anisotropies in particle momentum distributions
- Initial spatial anisotropy → Pressure gradient → Momentum space anisotropy
- Initial electromagnetic field → Directed flow

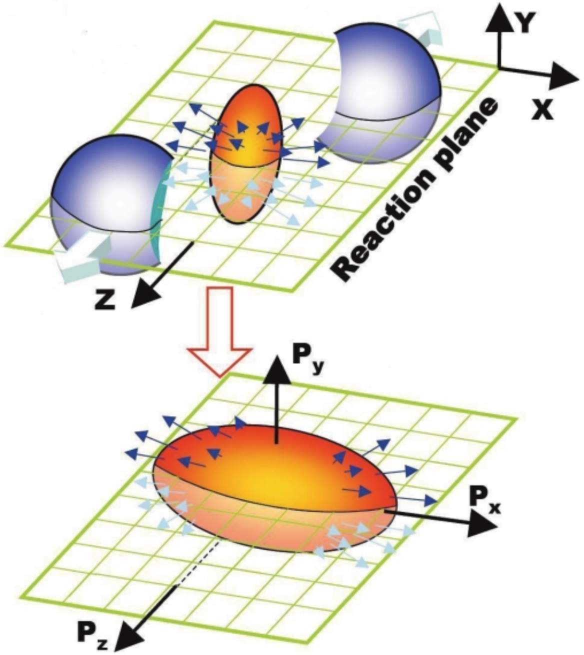

$$E\frac{d^3N}{dp^3} = \frac{1}{2\pi}\frac{d^2N}{p_T dp_T dy}\left(1 + \sum_{1}^{\infty} 2v_n \cos\left[n\left(\phi - \psi_r\right)\right]\right)$$

$$v_1 = \cos\left(\phi - \psi_r\right) = \left\langle \frac{p_x}{p_T} \right\rangle$$ directed flow

$$v_2 = \cos\left[2(\phi - \psi_r)\right] = \left\langle \frac{p_x^2 - p_y^2}{p_x^2 + p_y^2} \right\rangle$$ elliptic flow

1) Equation of State of the medium
2) Constituent interactions and degree of freedom

p_T dependence of v_1 slope at high μ_B

π^+, K^+, K^- and K_S^0

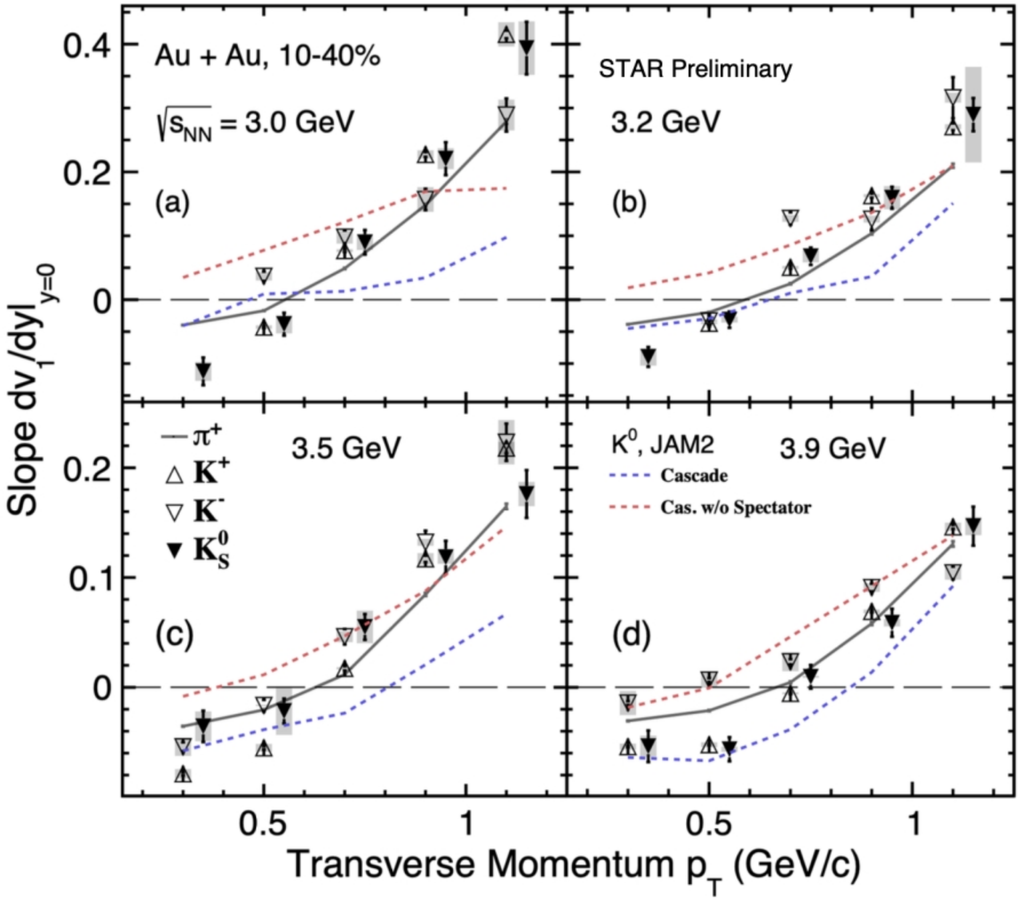

- Anti-fow of π^+ and K_S^0, $K^\pm$
- Anti-fow could be explained by shadowing effect from spectators

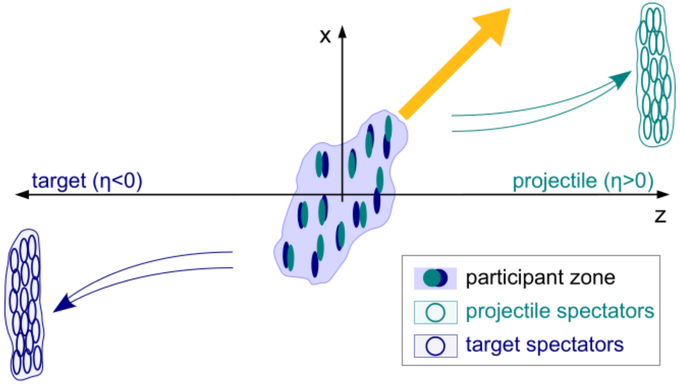

Energy dependence of nuclei <p_T>

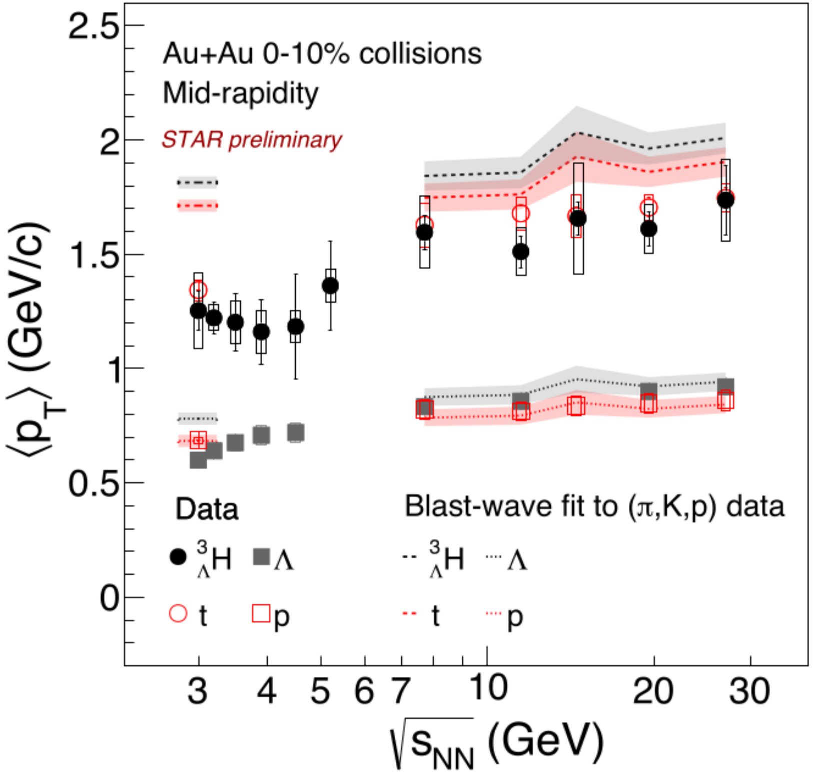

- Similar $\langle p_T \rangle$ for $^3_\Lambda$H and t
- Blast-wave fit using measured kinetic freeze-out parameters from light hadrons (π, K, p) **overestimates both $^3_\Lambda$H and t**

$^3_\Lambda$H and t do not follow same collective expansion as light hadrons. Can be interpreted as $^3_\Lambda$H and t decoupling at different times compared to light hadrons

- Different trend for $\sqrt{s_{NN}}$ = 3-4.5 GeV and $\sqrt{s_{NN}}$ = 7.7-27 GeV
  - Suggest different expansion dynamics?

Light nuclei collectivity vs energy

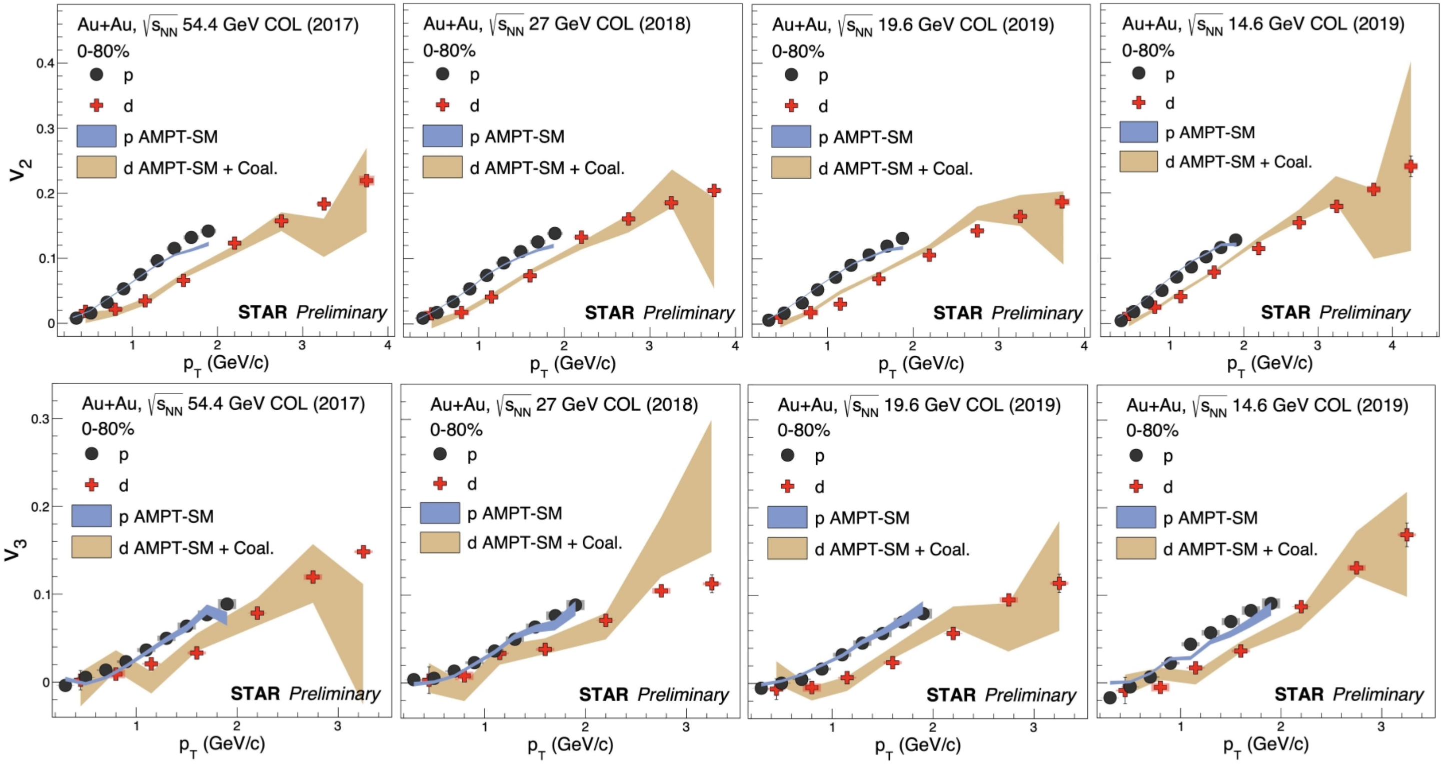

- ➔ **AMPT(SM) model with coalescence describes deuteron v_2 and v_3**
- ➔ **Insight into light nuclei production mechanism in HI collisions**

Light nuclei collectivity vs energy

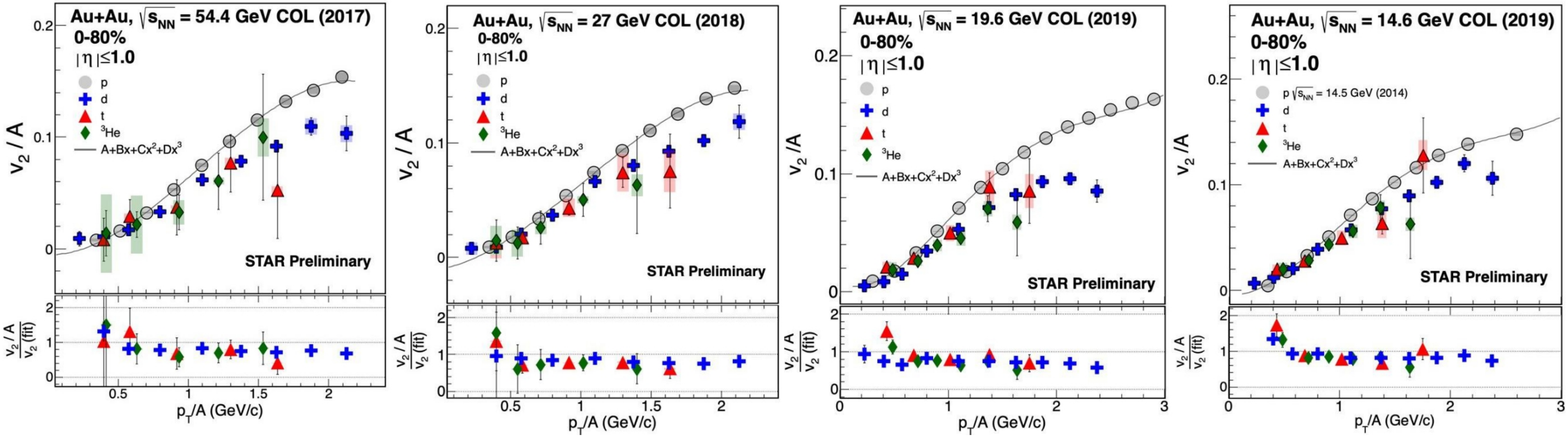

➔ **Light nuclei v_2 obeys mass number scaling at ~30% level in BES energies**

Directed flow of light and hyper nuclei at high μ_B

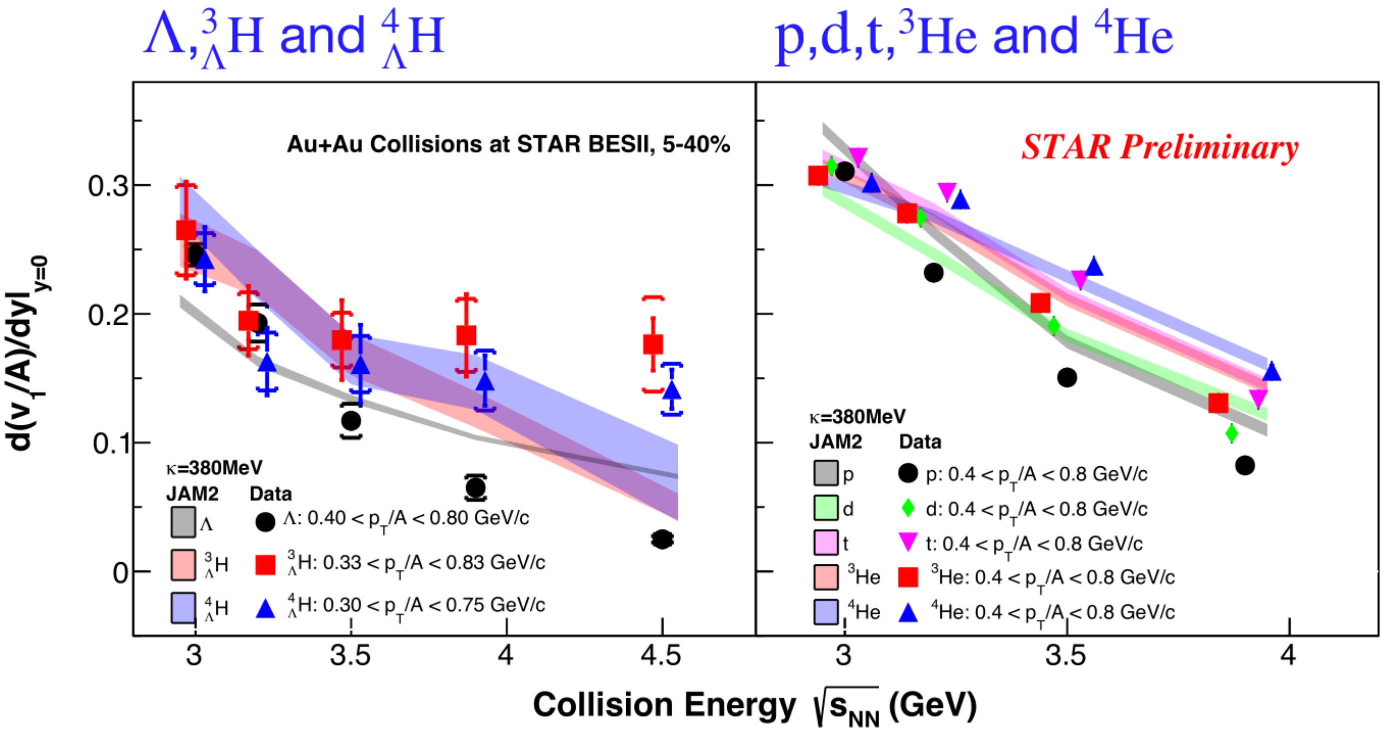

- v_1 slope: consistent with hadronic transport model (JAM2 mean field + Coalescence)
- Particle yields + $\langle p_T \rangle$ slope + v_1 slope support coalescence picture of light (hyper-)nuclei production

Energy dependence of S_3

- A prominent enhancement of the strangeness population factor S_3 was proposed as a probe for deconfinement

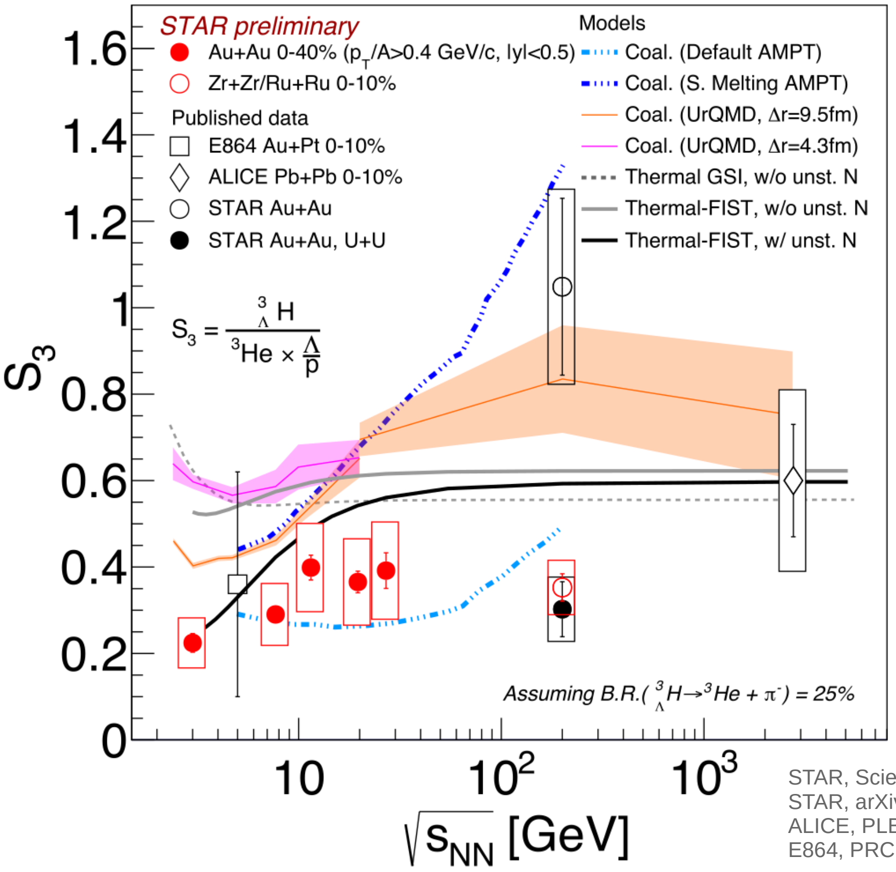

$$S_3 = \frac{^3_\Lambda \mathrm{H}}{^3\mathrm{He} \times \frac{\Lambda}{\mathrm{p}}}$$

- ➔ Data shows a mild increasing trend from s_{NN} = 3.0 GeV to 2.76 TeV
- ➔ Thermal-FIST, which includes feed-down from unstable nuclei to stable p, ^{3}He, describes the S_3 data better
  - ➔ Feed-down from unstable nuclei important

STAR, Science 328 (2010) 58
STAR, arXiv: 2310.12674
ALICE, PLB 754 (2016) 360
E864, PRC 70 (2004) 024902

A. Andronic et al, PLB 697 (2011) 203 (Thermal (GSI))
S. Zhang, PLB 684 (2010) 224 (Coal.+AMPT)
T. Reichert, et al, PRC 107 (2023) 014912 (UrQMD, Thermal-FIST)

${}^{3}_{\Lambda}H/\Lambda$ and S_3 dependence on the system size

- Measurement in isobar collisions at 200 GeV

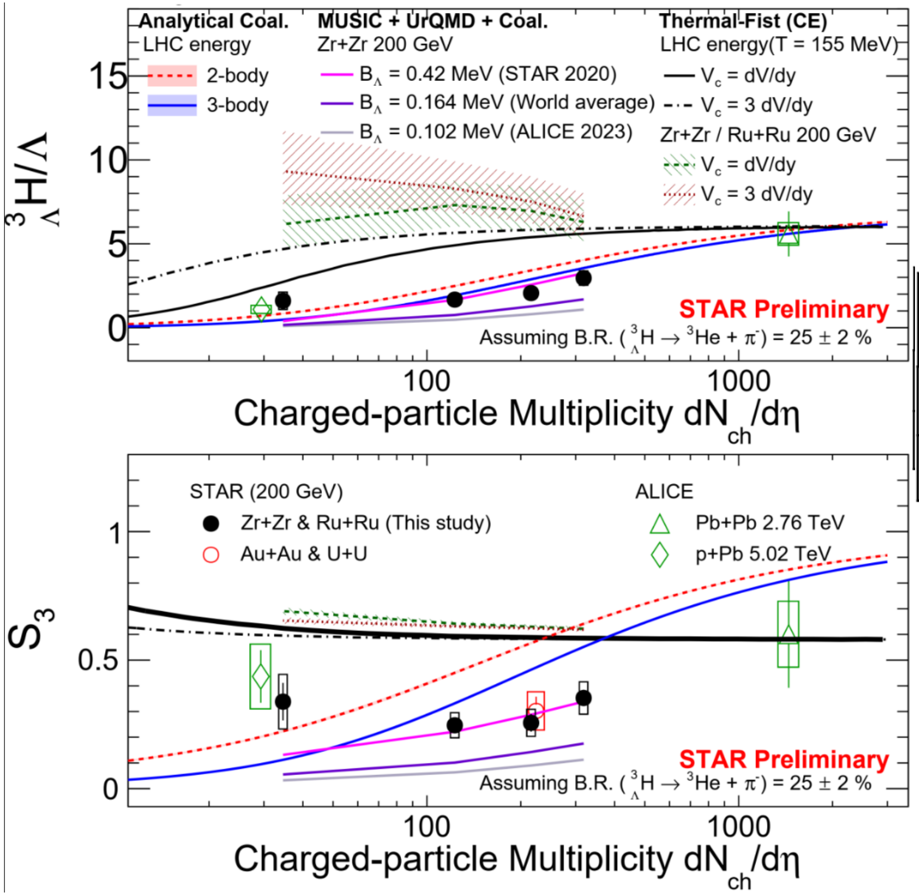

➔ STAR and ALICE data consistent

➔ Similar mechanisms for hypernuclei production at RHIC and LHC energies

Significance of deviation	Ana. coal. (2-body)	Ana. coal. (3-body)	MUSIC+UrQMD+Coal (average B_Λ)	Thermal
${}^{3}_{\Lambda}H/\Lambda$	3.8σ	1.9σ	3.8σ	$> 5\sigma$
S_3	6.6σ	3.9σ	3.6σ	$> 8\sigma$

Analytical Coalescence:
K.-J. Sun et.al., PLB 792, 132–137 (2019)
MUSIC + UrQMD + Coalescence:
K.-J. Sun et.al. arXiv:2404.02701
Thermal-Fist::
V. Vovchenko, H. Stoecker, Comput. Phys. Commun. 244, 295-310 (2019)

Baryon number carrier

Valence Quarks | **Junctions**

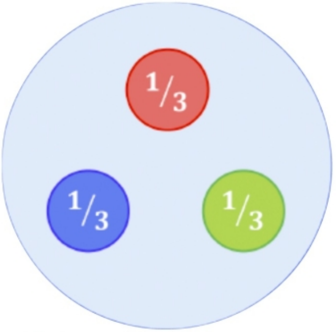

VS.

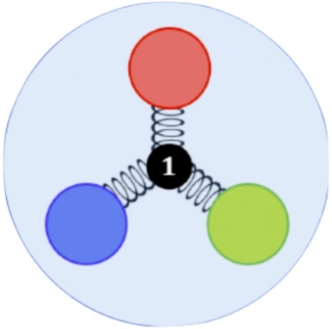

X. Artru, Nucl. Phys. B 85 (1975) 442
G. C. Rossi, G. Veneziano, Nucl. Phys. B 123 (1977) 507

- Carry large momentum fractions
- Hard to be stopped at midrapidity
  - $dN/d\Delta y \sim \exp(-2.4\Delta y)$ (PYTHIA)
  - $\Delta y = Y_{\text{beam}} - y$

VS.

- Consist of low-momentum gluons
- Easier to be stopped at midrapidity
  - $dN/d\Delta y \sim \exp(-0.5\Delta y)$ (theory)

Theory: D. Kharzeev, PLB 378 (1996) 238

Valence Quarks:

- $Q \sim B \times Z/A$

Junctions:

- $Q < B \times Z/A$

Baryon number carrier (2)

- Test 2: Net-proton dN/dΔy in γ+Au events
- Test 3: Net-proton vs. Rapidity Shift in Au+Au events

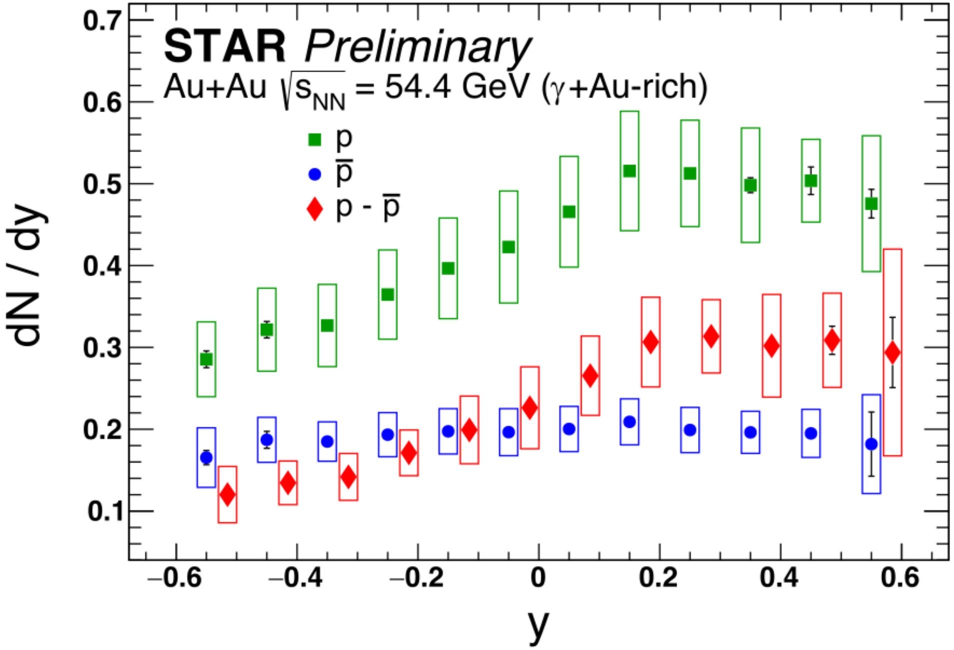

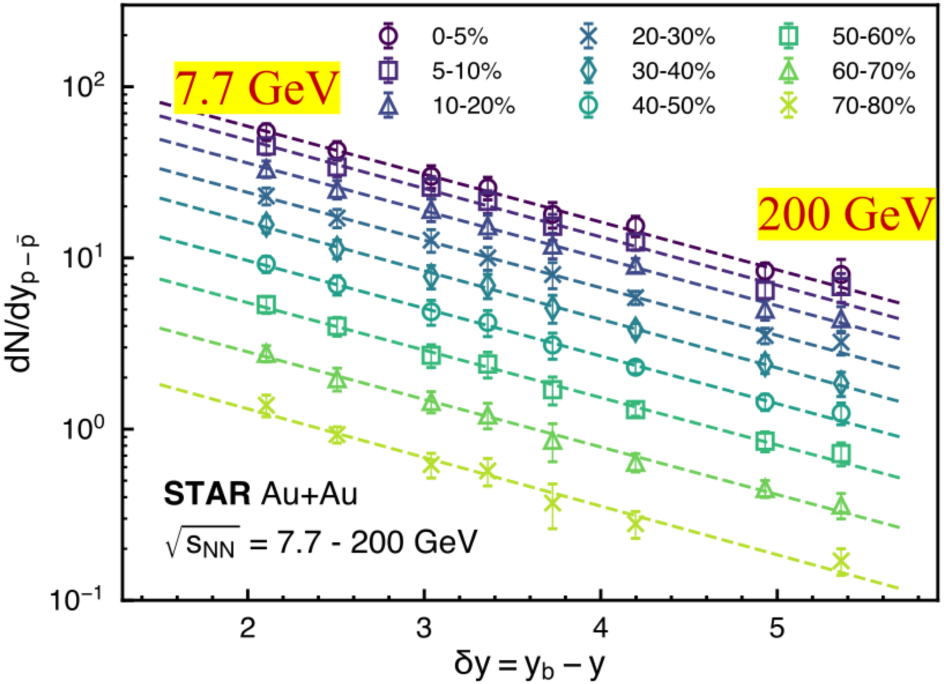

- Clear excess of p over anti-p → incoming photons can stop baryon number

γ+Au vs. Au+Au vs. Theory

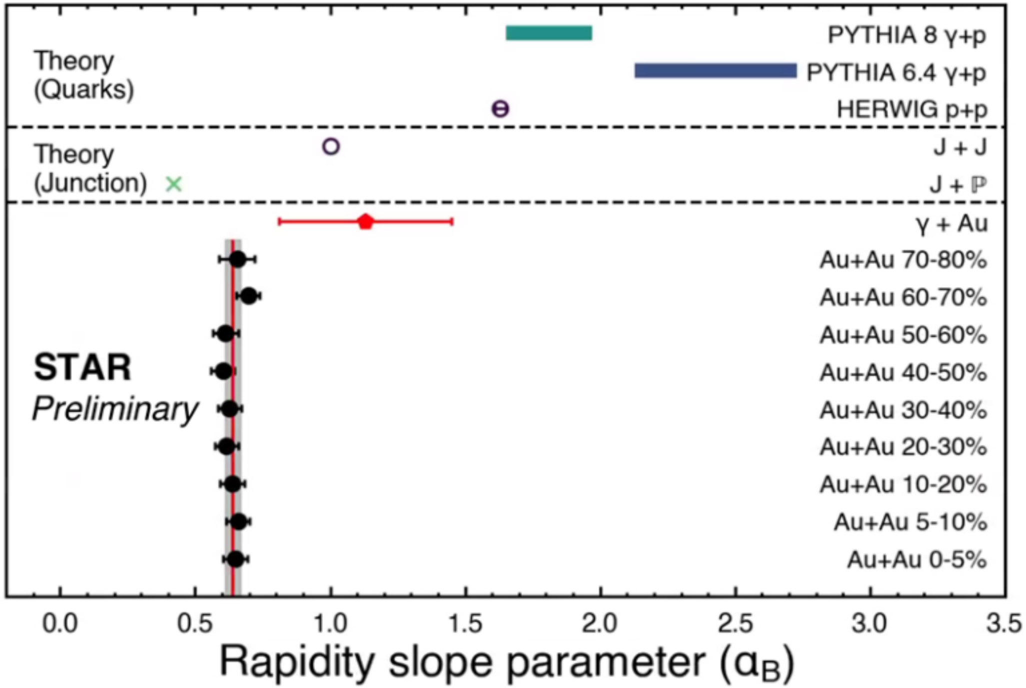

Junction theory: D. Kharzeev, PLB 378 (1996) 238

- No centrality dependence of the slope → not expected for valence quark stopping
- $Slope_{\gamma+\mathrm{Au}} >\sim Slope_{\mathrm{Au+Au}}$
- Qualitatively consistent with baryon junction prediction
- Smaller than HERWIG and PYTHIA predictions